Accepted Manuscript

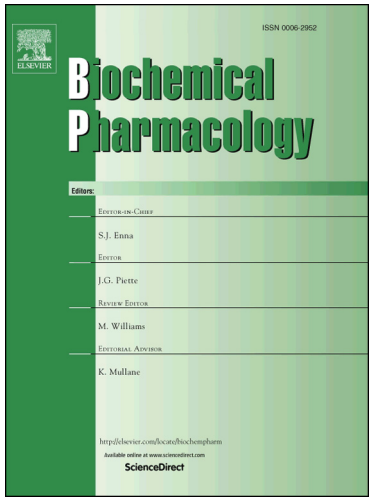

Effect of a long-term treatment with metformin in dystrophic *mdx* mice: a re-consideration of its potential clinical interest in Duchenne muscular dystrophy

Paola Mantuano, Francesca Sanarica, Elena Conte, Maria Grazia Morgese, Roberta Francesca Capogrosso, Anna Cozzoli, Adriano Fonzino, Angelo Quaranta, Jean-Francois Rolland, Michela De Bellis, Giulia Maria Camerino, Luigia Trabace, Annamaria De Luca

PII: S0006-2952(18)30165-5
DOI: https://doi.org/10.1016/j.bcp.2018.04.022
Reference: BCP 13131

To appear in: *Biochemical Pharmacology*

Received Date: 8 March 2018
Accepted Date: 19 April 2018

Please cite this article as: P. Mantuano, F. Sanarica, E. Conte, M.G. Morgese, R.F. Capogrosso, A. Cozzoli, A. Fonzino, A. Quaranta, J-F. Rolland, M. De Bellis, G.M. Camerino, L. Trabace, A. De Luca, Effect of a long-term treatment with metformin in dystrophic *mdx* mice: a reconsideration of its potential clinical interest in Duchenne muscular dystrophy, *Biochemical Pharmacology* (2018), doi: https://doi.org/10.1016/j.bcp.2018.04.022

Effect of a long-term treatment with metformin in dystrophic *mdx* mice: a reconsideration of its potential clinical interest in Duchenne muscular dystrophy.

Paola Mantuano[a], Francesca Sanarica[a], Elena Conte[a], Maria Grazia Morgese[b], Roberta Francesca Capogrosso[a], Anna Cozzoli[a], Adriano Fonzino[a], Angelo Quaranta[c], Jean-Francois Rolland[d], Michela De Bellis[a], Giulia Maria Camerino[a], Luigia Trabace[b] and Annamaria De Luca[a,*].

[a] *Section of Pharmacology, Department of Pharmacy - Drug Sciences, University of Bari "Aldo Moro", Bari Italy*

[b] *Department of Experimental and Clinical Medicine, Faculty of Medicine, University of Foggia, Foggia, Italy*

[c] *Department of Veterinary Medicine, University of Bari "Aldo Moro", Valenzano (BA), Italy*

[d] *Axxam, S.p.A, Openzone Science Park, Bresso (Milan, Italy)*

**Corresponding author at: Section of Pharmacology, Department of Pharmacy - Drug Sciences, University of Bari "Aldo Moro", Orabona 4 – Campus, 70125 Bari – Italy*

E-mail address: annamaria.deluca@uniba.it

Abstract

The pharmacological stimulation of AMP-activated protein kinase (AMPK) via metabolic enhancers has been proposed as potential therapeutic strategy for Duchenne muscular dystrophy (DMD). Metformin, a widely-prescribed anti-hyperglycemic drug which activates AMPK via mitochondrial respiratory chain, has been recently tested in DMD patients in synergy with nitric oxide (NO)-precursors, with encouraging results. However, preclinical data supporting the use of metformin in DMD are still poor, and its actions on skeletal muscle

appear controversial. Therefore, we investigated the effects of a long-term treatment with metformin (200mg/kg/day in drinking water, for 20 weeks) in the exercised *mdx* mouse model, characterized by a severe mechanical-metabolic maladaptation. Metformin significantly ameliorated histopathology in *mdx* gastrocnemius muscle, in parallel reducing TGF-β1 with a recovery score (r.s) of 106%; this was accompanied by a decreased plasma matrix-metalloproteinase-9 (r.s. 43%). In addition, metformin significantly increased *mdx* diaphragm twitch and tetanic tension ex vivo (r.s. 44% and 36%, respectively), in spite of minor effects on in vivo weakness. However, no clear protective actions on dystrophic muscle metabolism were observed, as shown by the poor metformin effect on AMPK activation measured by western blot, on the expression of mechanical-metabolic response genes analyzed by qPCR, and by the lack of fast-to-slow fiber-type-shift assessed by SDH staining in tibialis anterior muscle. Similar results were obtained in the milder phenotype of sedentary *mdx* mice. The lack of metabolic effects could be, at least partly, due to metformin inability to increase low *mdx* muscle levels of L-arginine, L-citrulline and taurine, found by HPLC. Our findings encourage to explore alternative, metabolism-independent mechanisms of action to differently repurpose metformin in DMD, supporting its therapeutic combination with NO-sources.

Key words: metformin, AMP-activated protein kinase, Duchenne muscular dystrophy, *mdx* mouse, skeletal muscle, chronic exercise.

Abbreviations

DMD, Duchenne muscular dystrophy; DGC, dystrophin-associated glycoprotein complex; ECM, extracellular matrix; SIRT1, Sirtuin1; PGC-1α, peroxisome proliferator-activated receptor γ coactivator 1α; PPARγ peroxisome proliferator-activated receptor γ; Bnip3, BCL2

interacting protein 3; NOX2, NADPH oxidase 2; Src-TK, c-Src tyrosine kinase; TNFα, tumor necrosis factor α; TGF-β1, transforming growth factor β1; AMPK, AMP-activated protein kinase; AICAR, 5-aminoimidazole-4-carboxamide-1-β-D-ribofuranoside; NO, nitric oxide; wt, wild type; DIA, diaphragm; EDL, extensor digitorum longus; TA, tibialis anterior; GC, gastrocnemius; MT, mechanical threshold; GAPDH, glyceraldehyde-3-phosphate dehydrogenase; ACTB, beta-actin; HPRT1, hypoxanthine-guanine phosphoribosyltransferase; UTRN, utrophin; Drp1, dynamin-related protein 1; Cox4i1, cytochrome C oxidase subunit IV isoform 1; Cs, citrate synthase; Lc3, microtubule-associated protein 1A/1B-light chain 3; SDH, succinate dehydrogenase; CK, creatine kinase; LDH, lactate dehydrogenase; MMP-9, matrix metalloproteinase-9; HPLC, High Performance Liquid Chromatography; HDAC, histone deacetylase.

1. Introduction

Duchenne muscular dystrophy (DMD) is a lethal X-linked muscle-wasting disorder with an average incidence of 1:5000 newborn males[1]. DMD is due to mutations in the gene encoding dystrophin, which cause the absence of the protein at subsarcolemmal level in striated muscle fibers[2]. In healthy muscle, dystrophin is part of the dystrophin-glycoprotein complex (DGC) and interacts with cytoskeletal components, forming a bridge between the intracellular cytoskeleton and the extracellular matrix (ECM). The lack of dystrophin is associated with the disorganization and degradation of the DGC and loss of mechanical stability and of proper intracellular signalling[3-5]. As a consequence, a complex cascade of events occurs and sustains the activation of pro-oxidative, pro-inflammatory and pro-fibrotic pathways, which finally lead to inefficient myofiber regeneration and progressive muscle wasting[2,4,6]. In the past decades, a major

contribution to the comprehension of DMD pathogenesis and assessment of potential therapies has been obtained with preclinical studies using the spontaneous dystrophic *mdx* mouse[7]. In line with the mechanical role of dystrophin, a standard protocol of chronic exercise on treadmill (*http://www.treatnmd.eu/research/preclinical/SOPs*) negatively affects the otherwise mild phenotype of *mdx* mice[8-13].

Recent genomic and proteomic studies support that part of the damaging effect of exercise is due to a failing mechanical-metabolic coupling in dystrophic myofibers. In fact, muscles of exercised *mdx* mice show a time-dependent downregulation of protective genes involved in metabolic adaptation to physical activity (SIRT1, PGC-1α, PPARγ), muscle repair (adiponectin, follistatin) and autophagy (Bnip3), which fails to contrast the overexpression of markers of oxidative stress (NOX2, Src-TK), inflammation (TNFα) and fibrosis (TGF-β1)[14,15]. Accordingly, a proteomic analysis underlined an increment in fast twitch fiber type proteins such as fast skeletal muscle troponins and myozenin-1) and glycolytic enzymes, accompanied by a reduction of key elements of mitochondrial respiratory chain and of energy metabolism (adenylate kinase)[16].

Interestingly, emerging therapeutic strategies for DMD are based on drugs acting as direct metabolic enhancers which would act as exercise mimetics without the damaging consequences induced by mechanical stress in dystrophin-deficient muscles. Similarly to what observed after the transgenic overexpression of PGC-1α[17-19], promising results have been obtained in dystrophic mice with the pharmacological stimulation of AMP-activated protein kinase (AMPK), a major metabolic sensor activated by increased AMP/ATP ratio, which activates the SIRT1-PGC-1α pathway[20]. Short term (4-week) treatments with the direct AMPK agonist AICAR (5-aminoimidazole-4-carboxamide-1-β-D-ribofuranoside) have been reported to increase both PGC-1α and utrophin expression in *mdx* myofibers and to improve mitochondrial function with a fast-to-slow phenotype switch, thereby

ameliorating muscle function and histology[21-23]. Building on these observations, it has been hypothesized that metformin, a first-line oral antidiabetic drug able to indirectly stimulate AMPK, would be beneficial for skeletal muscle function in DMD[24,25]. While first tested to control insulin resistance in a group of overweight, deflazacort-treated DMD boys[26], more recently metformin claimed direct attention for clinical studies in patients with DMD as disease modulator, in combination with amino acids sources of nitric oxide (NO) for a potential synergic action on muscle metabolism. The available results of the pilot study (NCT02516085), suggest that metformin and L-arginine treatment increased mitochondrial protein expression in vitro and in vivo and clinically delayed disease progression in DMD boys aged between 7-10 years[27,28]. However, preclinical data concretely supporting the efficacy of metformin by itself on disease progression are still poor. Langone et al. observed an enhanced protection against cardiotoxin injury in muscles of metformin-treated mice[29]. In 2015, Ljubicic and colleagues described the ability of metformin to increase PGC-1α and utrophin A protein expression in vitro (in C_2C_{12} muscle cells) and in vivo[30]. However, these latter experiments have been performed for a short term (6 weeks) and in non-exercised *mdx* mice, which already show a basal overexpression of genes involved in the metabolic protection[14,16]. The questioning about metformin efficacy mainly resides on the available evidences about its mechanism of action. In fact, metformin has been proposed to stimulate metabolism primarily by inhibiting complex I in mitochondria, a pathway that is already impaired in either sedentary or chronically exercised *mdx* mice and in DMD patients[16,31,32]. The present study has been aimed at assessing the effect of a long-term treatment with metformin (20 weeks) in exercised *mdx* mouse model on dystrophy-related in vivo and ex vivo primary endpoints. This in order to increase our knowledge on the drug mechanisms

of action and to verify its potential efficacy as metabolic enhancer in a more severe metabolic state of dystrophic muscle, more closely resembling that of DMD patients.

2. Materials and methods

All experiments were conducted in conformity with the Italian law for Guidelines for Care and Use of Laboratory Animals (D.L. 116/92) and with the European Directive (2010/63/UE). The study has been approved by national ethic committee for research animal welfare of the Italian Ministry of Health (protocol number: DGSAF0024012). Most of the experimental protocols used conform to the standard operating procedures (SOPs) for preclinical tests in *mdx* mice, available on the TREAT – NMD website (*http://www.treat-nmd.eu/research/preclinical/dmd-sops/*).

2.1 In vivo procedures

2.1.1 Animal groups, protocols of exercise and drug treatment

A group of 13 male *mdx* mice (C57BL/10ScSn-*Dmd*^{mdx}/J) of 4-5 weeks of age were purchased from The Jackson Laboratory (USA, distributed by Charles River, Italy). Mice were acclimatized for one week in the animal facility prior to the beginning of the protocol; then, they were segregated into different cages based on their body weight and subsequently randomly assigned to metformin-treated and untreated subgroups. A group of age- and sex-matched wild type mice (wt, C57BL/10ScSn/J; n = 6), taken as sedentary, was used as control.

Every week, all mice were monitored for body weight and forelimb force by means of a grip strength meter (Columbus Instruments, Columbus, Ohio, USA). Values of both absolute and normalized (to body weight) maximal forelimb force obtained at the main

time points (every 4 weeks, from T0 to T20) were used for statistical analysis. Exercised *mdx* mice underwent a protocol of 30-minute running on a horizontal treadmill (Columbus Instruments, Columbus, Ohio, USA) at 12 m/min twice a week, keeping a constant interval of 48-72 hours between exercise sets[8,9,33]. In addition, every four weeks all experimental groups underwent an acute exercise resistance test on treadmill to evaluate in vivo fatigue[9,34].

For a better evaluation of drug outcome on our model, a total of 16 age- and sex-matched sedentary *mdx* mice (divided in 9 untreated and 7 metformin-treated animals) were added to our study. These mice underwent the same in vivo and ex vivo procedures of the above described experimental groups.

Metformin hydrochloride (1-dimethylbiguanide hydrochloride, Sigma – Aldrich, MO, USA) was formulated in filtered tap water and administered orally at a dose of 200 mg/kg/day. The dose was adjusted according to weekly water consumption *per* cage, which was calculated by measuring the volume of water at the end of each week, divided for the number of mice/cage and normalized to the mean body weight of the mice in the cage. The dose of metformin was chosen converting the human dose in the appropriate animal equivalent dose and on the basis of previous preclinical studies in dystrophic mice[29,30,35], in order to be in the optimal therapeutic range and in parallel to avoid toxicity. The duration of the treatment was 20 weeks in order to evaluate the effects of metformin in a more severe pathological condition of *mdx* mice due to long-term chronic exercise[14,15]. The treatment started one day before the beginning of the exercise protocol and continued until the day of sacrifice for ex vivo experiments.

For the whole duration of the study, regular light-dark cycles were maintained, and functional tests were performed during the light cycle phase. All mice were maintained on a controlled diet, with a daily amount of chow of 4-5 g/mouse (composition described in

[36]). No unusual behavior or macroscopic alteration of vital functions were observed in treated mice with respect to untreated counterparts. Also, no signs of stress (body weight loss, hair loss, lack of appetite, stereotypic or aggressive behavior, etc.) were ever observed. Due to the time-consuming nature of ex vivo procedures, a maximum of two mice *per* day were sacrificed. Thus, a window of 2-3 weeks for these experiments with consequent additional exercise/treatment was used.

2.2 Ex vivo procedures

2.2.1 Muscle preparations

All mice were anaesthetized intraperitoneally with a combination of ketamine (100 mg/kg) and xylazine (16 mg/kg); a lower dose of ketamine alone (30mg/kg) was additionally administered to ensure a longer and deeper sedation, if required. This procedure was necessary to guarantee a normal blood circulation during muscle excision so to preserve unaltered the functional characteristics of muscle tissue.

Several muscles were dissected from each mouse and then used for the planned endpoint assessments, according to our previous experiments and the guidelines described by Willmann et al., 2012[9,13-15,36,37], also in order to fulfil the 3Rs requirements about ethical animal use.

A strip of right hemi-diaphragm (DIA) and the *extensor digitorum longus* (EDL) muscle of the left hind limb from wt and *mdx* mice, were carefully removed with tendons intact on both ends and rapidly placed in chambers for isometric and/or eccentric contraction recordings. The EDL muscle of the right hind limb was removed and placed in a bath for microelectrodes electrophysiological recordings. Tibialis anterior (TA) and gastrocnemius (GC) muscles from one hind limb were dissected, embedded in a small amount of Tissue – Tek O.C.T. (Bio – Optica, Milan, Italy) and immersed in isopentane cooled with liquid

nitrogen for 20-40 seconds; frozen samples were stored at -80°C until further processed for histological analysis. Contralateral GC muscles were snap frozen in liquid nitrogen and stored at -80°C until used for Real-time PCR experiments and TGF-β1 ELISA test. Contralateral TA muscles were cut in half; one half was snap frozen in liquid nitrogen and stored at -80°C until use for western blot. The other half was weighed and immediately homogenized in 0.1N perchloric acid using Potter-Elvehjem glass tissue homogenizers. Homogenized tissue was then centrifuged at 12000 rpm for 60 minutes at 4°C and the surnatant was stored at -80°C for further HPLC (High Performance Liquid Chromatography).

2.2.2 Isometric and eccentric contraction recordings on isolated muscles

EDL muscle was securely tied with silk suture 6-0 to the proximal and distal tendons during dissection, and then gently removed from the mouse. A strip of diaphragm, no more than 4 mm wide, was cut from the excised muscle and then tied firmly at the rib and the central tendon[38]. For each muscle, two loops were made at the end of the sutures to allow the placement into a muscle bath containing 25 ml of Ringer's solution, an isotonic solution with the following composition (in mM): NaCl 148, KCl 4.5, $CaCl_2$ 2.0/2.5, $MgCl_2$ 1.0, NaH_2PO_4 0.44, $NaHCO_3$ 12.0, glucose 5.55, pH 7.2 – 7.4, continuously gassed with a mixture of 95% O_2 and 5% CO_2 and maintained at 27 ± 1°C. The EDL muscle was placed in a horizontal bath (mod. 809B-25, ASI, Aurora, Ontario, Canada), fixed by one tendon to the chamber hook, while the other tendon was fixed to a Dual-Mode Lever System 1N force transducer (mod. 300C LR, ASI), connected to a proper interface and data acquisition system (Dynamic Muscle Control v5.415, ASI). The diaphragm strip was placed in a vertical muscle bath, with the central tendon fixed to the chamber hook, and the rib fixed to a force transducer (FORT25, WPI Inc, Florida, USA), connected to a TCI 102 interface with a MP100 acquisition unit and AcqKnowledge v.3.8 software (Biopac

Systems, Santa Barbara, CA, USA). In both chambers, electrical field stimulation was obtained by two axial platinum electrodes closely flanking the muscles and connected to a stimulator (EDL: 701C High-Power, Bi-Phase Stimulator, ASI; DIA: LE 12406, 2Biological Instruments, VA, Italy). After a 30-minute equilibration in the bath, the preparations were stretched to their optimal length (L0), measured with an external calliper. L0 represents the length producing the maximal single contraction (twitch) in response to a 0.2 ms square wave 40-60 mV pulse. Maximal twitch tension was obtained as the mean value from 5 single twitches elicited by pulses of 0.2 ms, every 30 seconds. Tetanic contractions were elicited by applying trains of 350 ms and 450 ms (for EDL and DIA, respectively) of 2.0 ms pulses at increasing frequencies (10-250 Hz), every 2 minutes. The maximal tetanic force was usually recorded at 140-180 Hz for EDL, and at 120-140 Hz for DIA. At last, EDL muscles underwent a protocol of 10 eccentric contractions, elicited at 120 Hz for 500ms every 30 seconds. For each stimulus, the initial 300 ms stimulation was isometric, followed by a stretch of 10% L0 at a speed of 1L0 s^{-1} imposed for the last 200 ms. The progressive decay in isometric force at 5^{th} and 10^{th} pulse was calculated as percent reduction with respect to the force value at first pulse. Two tetanic isometric contractions (120 Hz, 500ms) were elicited at 4 and 30 minutes after the eccentric contractions protocol to estimate muscle recovery from the stretch-induced force drop compared to the tetanic force registered before the protocol started. At the end of the experiments, tendons were removed, and the muscles were blotted dry with filter paper; then, their mass was determined for subsequent data normalization. Data were analysed using AcqKnowledge software v3.8 (Biopac Systems) for DIA and Dynamic Muscle Analysis software v5.201 (ASI) for EDL, to obtain muscle contraction kinetics (time to peak twitch and half relaxation time, in ms) and absolute values of maximal twitch (Ptw) and tetanic (P0) tension. Absolute values were normalized by muscle cross sectional area

according to the equation sP = P/(Mass/Lf*D) where P is absolute tension, Mass is the muscle mass, D is the density of skeletal muscle (1.06 g/cm^3), Lf was determined by multiplying L0 by previously determined muscle length to fiber length ratios (DIA = 1; EDL = 0.44)[12,15,39,40].

2.2.3 Electrophysiological recordings by intracellular microelectrodes

EDL muscle was bathed at 30 ± 1°C into a chamber containing 25 ml of 95% O_2-5% CO_2-gassed Ringer's solution. A two microelectrode "point" voltage clamp method was used to determine the mechanical threshold (MT) for contraction of EDL muscle fibers in the presence of tetrodotoxin (3 µM)[9,41,42]. In brief, the two microelectrodes (spaced about 50 µm) were inserted into the central region of a superficial fiber, continuously viewed using a stereomicroscope (100x magnification). Depolarizing command pulses of duration ranging from 500 to 5 ms (0.3 Hz) were progressively increased in amplitude from the holding potential (H) of -90 mV until visible contraction. The threshold membrane potential (V, in mV) was read on a digital sample-and-hold millivoltmeter for each fiber at the various pulse durations t (in ms); mean values at each t allowed the construction of a "strength-duration" curve. Rheobase voltage (R, in mV) and the rate constant ($1/\tau$, sec^{-1}) to reach the rheobase were obtained by a non-linear least square algorithm using the following equation: $V = (H - R \exp(t/\tau))/(1 - \exp(t/\tau)$[9,41,42].

2.2.4 Protein expression analysis by western blot

Protein extraction and immunoblot for the determination of phosphorylated AMPK/AMPK were conducted as described in previous work[15,43], on TA muscles from wt and *mdx* mice, both sedentary and exercised. Briefly, portions of TA muscles were homogenized in ice cold buffer containing 20 mM Tris-HCl (pH 7.4 at 4°C), 2% SDS, 5 mM EDTA, 5 mM EGTA, 1 mM dithiothreitol, 100 mM NaF, 2 mM sodium vanadate, 0.5 mM phenylmethylsulfonyl fluoride, 10 mg/mL leupeptin and 10 mL/mL pepstatin.

Homogenates were centrifuged at 1500 g for 5 min at 4°C. The supernatant obtained was quantified using Bradford protein assay kit (Bio-Rad Protein Assay Kit I5000001, Bio-Rad, CA, USA). 40 µg of proteins were separated on a 10% SDS-PAGE and transferred on to nitrocellulose membranes for 1 h at 150 mA (SemiDry transferblot; Bio-Rad). Membranes were blocked for 2 h with Tris-HCl 0.2 M, NaCl 1.5 M, pH 7.4 buffer (TBS) containing 5% non-fat dry milk and 0.5% Tween 20 (Bio-Rad), incubated overnight at 4°C with primary antibodies. The following dilution of primary antibodies were used: AMPK (rabbit polyclonal, Cell Signaling Technology Inc., MA, USA) 1:1000, phosphorylated AMPK (rabbit polyclonal, CST) 1:1000 with TBS containing 5% non-fat dry milk. After three washes with TBS containing 0.5% Tween 20 (TTBS), membranes were incubated for 1 h with secondary antibody labeled with peroxidase (1:5000 anti-rabbit IgG, Sigma – Aldrich, MO, USA). Membrane was then washed with TTBS, developed with a chemiluminescent substrate (Clarity Western ECL Substrate, Bio-Rad) and visualized on a Chemidoc imaging system (Bio-Rad). Densitometric analysis was performed using Image Lab software (Bio-Rad). The software allows the chemiluminescence detection of each experimental protein band to obtain the absolute signal intensity. The density volume was automatically adjusted by subtracting the local background. Due to the potential high inter-individual variability, 6 – 7 mice per group were analyzed. The large number of samples made it necessary to carry out at least four independent western blot experiments, in each of which all the experimental conditions of interest were represented. The quality of protein loading and transfer has been assessed with red Ponceau staining on each PVDF membranes[15].

2.2.5 Isolation of total RNA, reverse transcription and Real-time PCR

Real-time PCR experiments were performed according to the MIQE guidelines for qPCR, as published[44]. Total RNA was isolated from GC muscles by RNeasy Fibrous Tissue

Mini Kit (Qiagen, Valencia, CA, USA; C.N.74704) and quantified by spectrophotometry (ND-1000 NanoDrop, Thermo Scientific, Waltham, MA, USA). Reverse transcription was performed as described in detail in previous work[14,15]. Real-time PCR was performed by using the Applied Biosystems® Real-Time PCR 7500 Fast system (Thermo Fisher Scientific). Each reaction, carried out in triplicate, consisted of 8 ng of cDNA, 0.5 µl of TaqMan Gene Expression Assays, 5 µl of TaqMan Universal PCR master mix No AmpErase UNG (2x) (C.N. 4324018) and Nuclease-Free Water not DEPC220 treated (C.N. AM9930; all from Thermo Fisher Scientific) for a final volume of 10 µl. RT - TaqMan - PCR conditions were: step 1: 95°C for 20 s; step 2: 95°C for 3 s; step 3: 60°C for 30 s; steps 2 and 3 were repeated for 40 times. Results were compared with a relative standard curve obtained from 5 points of 1:4 serial dilutions. The mRNA expression of genes was normalized to the best housekeeping gene glyceraldehyde-3-phosphate dehydrogenase (GAPDH), selected from beta-actin (ACTB), GAPDH and hypoxanthine-guanine phosphoribosyltransferase (HPRT1) by GenNorm software. TaqMan hydrolysis primer and probe gene expression assays (Thermo Scientific) were ordered with the following Assay Ids: *GAPDH*: Mm99999915_g1; *HPRT1*: Mm00446968_m1; *ACTB*: Mm00607939_s1; Peroxisome proliferative activated receptor γ coactivator 1α (*PGC-1α*): Mm01208835_m1; Sirtuin1 (*SIRT1*): Mm00490758_m1; Peroxisome Proliferator Activated Receptor γ (*PPARγ*): Mm01184322_m1; Peroxisome Proliferator Activated Receptor β/δ (*PPAR β/δ*): Mm00803184_m1; Utrophin (*Utrn*): Mm01168866_m1; cSrc Tyrosine Kinase (*Src-TK*): Mm 00432751 m1; Dynamin-Related Protein 1 (*Drp1*): Mm01342903; Cytochrome C oxidase subunit IV isoform 1 (*Cox4i1*): Mm01250094_m1; Citrate synthase (*Cs*): Mm00466043_m1; BCL2 interacting protein 3 (*Bnip3*): Mm01275600_g1. For microtubule-associated protein 1A/1B-light chain 3 (*Lc3*) the assay was made with: forward primer 5′-ATCCCAGTGATTATAGAGCGATACAA-3′, reverse

primer 5′-TCAGGCACCAGGAACTTGGT-3′, and probe 6-FAM-AGA AGC AGC TGC CCG-MGB to amplify the mRNA with NCBI Reference Sequence number NM_026160.4.

2.2.6 Muscle histology and histochemistry

Frozen GC and TA muscle samples were placed at -20°C into the cryostat (HM 525 NX, Thermo Fisher Scientific, MA, USA) for at least 20 minutes before further processing. 6-7 μm thick GC muscle sections were transversally cut and stained with hematoxylin/eosin to calculate the total area of damage (necrosis, inflammation and non-muscle areas) as well as the percentage of regenerating/regenerated myofibers, showing central nuclei (centrally nucleated fibers). 10 μm fresh-frozen, transversally cut TA muscle sections were stained to evaluate the relative succinate dehydrogenase (SDH) of individual myofibers and to demonstrate changes in the overall oxidative capacity of the muscle.

Morphological features of the muscles related to each type of staining were identified using digital images of stained sections, acquired using a bright-field microscope (CX41, Olympus, Rozzano, Italy) and an image capture software (Image J, Olympus). Morphometric analysis was performed on at least 3 fields from each muscle section and at least 5 animals *per* group were assessed.

2.2.7 Evaluation of biomarkers of muscle damage and determination of plasma glucose

Blood was obtained from cardiac puncture of left ventricle with a heparinized insulin syringe and collected in heparinized tubes. The samples were processed within 30 minutes after collection. Platelet-poor plasma was obtained after a first centrifugation step (20 mins at 4000 rpm at 4°C) to remove almost all corpuscolate elements of the blood; a second centrifugation step (10 minutes at 12000 rpm) was performed to ensure complete platelet removal. Creatine kinase (CK), lactate dehydrogenase (LDH) and glucose levels in plasma samples were determined by means of a spectrophotometer, using specific kits

(CK NAC LR, LDH LR and Glucose LR, SGM Italy). For both CK and LDH assays, the instrument was set to a wavelength of 340nm, at a temperature of 37°C; for glucose assay the wavelength was of 510nm.

The endopeptidase matrix metalloproteinase-9 (MMP-9) was measured in 20-fold diluted plasma samples by enzyme-linked immunosorbent assay (Quantikine® ELISA Mouse Total MMP-9 Immunoassay, R&D Biosystems, MN, USA), according to the manufacturer's instructions. The optical density of each well was determined, using a microplate reader set to 450 nm (Victor 3V, Perkin Elmer). A standard curve was generated for relative quantification. MMP-9 levels were expressed in ng/ml. Total TGF-β1 protein was also measured by ELISA, (Quantikine® ELISA Mouse TGF-β1 Immunoassay, R&D Biosystems). Briefly, frozen GC muscle tissue (10-20 µg) was homogenized in 500 µl of a solution with the following composition: 20 mM TRIS (pH 8.0), 1% Triton X-100, 137 mM sodium chloride, 10% glycerol, 5 mM ethylenediaminetetraacetic acid and 1 mM phenyl methyl sulphonyl fluoride. TGF-β1 levels were expressed as pg of TGF-β1/µg of total protein content[13, 15].

2.2.8 Quantification of citrulline, arginine and taurine by HPLC

Amino acid concentrations were determined by HPLC using LC18 reverse phase column (Kinetex, 150 mm×3 mm, ODS 5 µm; Phenomenex, Castel Maggiore, Bologna, Italy) with fluorescence detection after derivatization with ophthalaldehyde/mercaptopropionic acid (emission length, 4.60 nm; excitation length, 3.40 nm), as previously described[45]. The mobile phase gradient consisted of 50mM sodium acetate buffer, pH 6.95, with methanol increasing linearly from 2 to 30% (v/v) over 40 min. The flow rate was maintained by a pump (JASCO, Tokyo, Japan) at 0.5 ml/min. Results were analyzed by Borwin software (version 1.50; Jasco) and substrate concentration was expressed as µM.

Dilution factor for taurine was 1:11.000, while citrulline and arginine dilution factor was set at 1:100.

2.3 Statistical analysis

All experimental data were expressed as mean ± standard error of the mean (S.E.M.). The S.E. estimate for the fitted rheobase (and relative statistical analysis) were obtained as described previously[9,33,41]. Multiple statistical comparisons between groups were performed by one-way ANOVA, with Bonferroni's t test post hoc correction when the null hypothesis was rejected ($p < 0.05$), to allow a better evaluation of intra- and inter-group variability and avoiding false positive[12,46]. If necessary, single comparisons between two means were performed by the unpaired Student's t-test. The recovery score, an objective index which allows to assess the effect of drug treatments on a given parameter, was calculated according to Standard Operating Procedures (SOPs) described in the TREAT – NMD website (*http://www.treat-nmd.eu/research/preclinical/dmd-sops/*) as follows:

Recovery score = [mdx treated] − [mdx untreated] / [wild type] − [mdx untreated] × 100

3. Results

3.1 Effect of metformin on in vivo and ex vivo functional parameters

All mice were monitored for body weight and in vivo forelimb force. These measurements started at the beginning of the treatment (T0) and continued until the day of sacrifice; the end of the 20th week (T20) was considered as the final time point for statistical analysis. The time-dependent effect of chronic treadmill exercise on body weight and forelimb force in the *mdx* mouse model has been extensively described[9,12-15]. Accordingly, an age-

and genotype-dependent increase in body weight was observed in all the experimental groups, with *mdx* mice being heavier than wt ones (Figure 1A). The treatment with metformin did not induce any significant change in body weight of exercised *mdx* mice (Figure 1A). In line with previous studies, values of both absolute and normalized (to body weight) forelimb grip strength of *mdx* mice groups were markedly lower than those of wt mice (Figure 1B, C). Metformin-treated exercised *mdx* mice tended to have a moderate increase in normalized force values compared to those of untreated ones at the main time points, showing a statistical significant increase only at T16 (Figure 1C). No protective effect of the drug was observed on exercise performance during the exhaustion test on treadmill (data not shown).

At the end of the 20-week treatment protocol, ex vivo isometric and eccentric contraction recordings of isolated diaphragm (DIA) and EDL muscle were performed. Metformin was effective in significantly improving specific twitch and tetanic force in DIA from exercised *mdx* mice with respect to untreated ones, with a recovery score versus wt values of 44% and 36%, respectively (Figure 2A, B). No protective effect of metformin was instead observed on isometric contraction of EDL muscles of dystrophic mice, with a poor recovery score (12%) for tetanic tension (Figure 2C, D). No effect by metformin was observed on contraction kinetics of either DIA or EDL muscle (Table 1). Also, neither EDL muscle force drop during eccentric contraction, nor the recovery from it, were ameliorated by the drug.

In parallel, the effects of metformin were also evaluated on excitation-contraction coupling of EDL muscle myofibers by means of voltage-clamp recordings of the mechanical threshold (MT), i.e. the voltage threshold for myofiber contraction. A shift of MT toward more negative potentials is a hallmark of EDL muscle fibers in dystrophic mice[9]. The impact of metformin treatment on MT is reported in Figure 3. As can be seen,

the strength-duration curve of EDL muscle fibers from metformin-treated *mdx* mice was significantly shifted toward more positive potentials at most of pulse durations (Figure 3). The MT rheobase voltage of metformin-treated muscles was slightly shifted to - 67.5 ± 2.2 mV, with respect to the value of - 71.6 ± 1.6 mV of untreated ones; the recovery score toward wt value (- 63.9 ± 2.1 mV) was of 15%.

3.2 Modulation of protein and gene expression by metformin treatment

In relation to the molecular mechanism of action of metformin[25], the ratio between phosphorylated AMPK (pAMPK)/AMPK was assessed by western blot in TA muscle samples (Figure 4A, B, C). In line with our recent results[15], the pAMPK/AMPK ratio was higher in TA muscles from exercised *mdx* mice groups with respect to wt animals, although not significantly (Figure 4C). Interestingly, the treatment with metformin induced a trend toward a further increase in the pAMPK/AMPK ratio of exercised *mdx* mice compared to untreated ones (+13.5%) and the ratio became significantly higher than that found in wt animals (Figure 4C).

To evaluate whether metformin was able to modulate the expression of genes related to the dystrophic condition and/or to metabolism, a panel of Real-time PCR experiments was performed on GC muscle samples. The results are shown in Figure 5. The long-term treatment with metformin in parallel with chronic exercise in *mdx* mice did not significantly modulate the expression of exercise-sensitive genes involved in AMPK signaling, such as SIRT1and PGC-1α, as well as of their downstream targets PPARγ and PPARβ/δ. In parallel, no significant alteration was found in expression of DRP1, a marker of mitochondrial fission, as well as of citrate synthase (Cs) and Cox4, oxidative energy metabolism markers and indices of mitochondrial biogenesis. Accordingly, metformin induced only a slight, not significant, increase in the gene expression of utrophin, a PGC-

1α target, with respect to vehicle. In parallel, a trend toward reduction of the redox-sensitive c-Src tyrosine kinase was observed in treated animals, while the drug modestly modulated the expression of the autophagy markers Lc3 and Bnip3 (Figure 5).

3.3 Drug-specific effects on dystropathology and biomarkers of muscle damage

3.3.1 Muscle histopathology and histochemistry

The effect of metformin on muscle histopathology was assessed on hematoxylin & eosin-stained GC muscle sections from the different experimental groups. The typical hallmarks of dystrophic histopathology were clearly present in both *mdx* sections, characterized by the alteration of myofiber architecture, with areas of necrosis, muscle infiltrates and non-muscle areas likely due to the deposition of fibrotic and adipose tissue, as well as by the presence of centronucleated myofibers, an index of degeneration/regeneration cycles (Figure 6A). Since *mdx* muscles are characterized by a high inter-individual variability and often by a great variability within different fields from the same sample[12,15,33,36,47], a morphometric analysis was performed to obtain quantitative data about the histological changes in each experimental group. As can be seen in Figure 6B, untreated *mdx* muscles showed a significantly higher percentage in the total area of damage (considered as the sum of necrosis, infiltration and non-muscle area) with respect to wt, as well as observed specifically for non-muscle area. Interestingly, metformin significantly reduced both the percentage of total damage and non-muscle tissue in exercised *mdx* muscles, compared to untreated ones (Figure 6B), while no difference in the content of centronucleated fibers was found between treated (62.3 ± 4.1%; n = 6) and untreated (63.3 ± 1.5%; n = 10) mice. To gain more insight into the role of metformin as a modulator of muscle metabolism, we investigated the potential ability of the drug to promote a fast-to-slow fiber type switch in dystrophic TA muscle sections by a succinate dehydrogenase (SDH) assay. As shown in Figure 6C, the SDH stain allows to distinguish between myofibers with high oxidative

capacity and less oxidative/non-oxidative fibers, with type I oxidative myofibers typically appearing darker than those of type II. Quantitative analysis confirmed no significant differences in myofiber composition among the experimental groups and the absence of a phenotype switch in metformin-treated animals (Figure 6D).

3.3.2 Effect of metformin on muscle TGF-β1 and plasma biomarkers of muscle sufferance

To assess the impact of metformin treatment on *mdx* muscle fibrosis, the expression of cytokine TGF-β1, a key pro-fibrotic biomarker, was measured by ELISA in GC muscle samples from exercised *mdx* mice, either treated or not, compared to wt (Figure 7A). As expected, the level of TGF-β1 was significantly higher in vehicle-treated *mdx* mice versus wt[15]. Metformin lead to a significant decrease of the fibrotic cytokine in exercised dystrophic mice (recovery score: 106%), showing a positive correlation with histopathology results. Another marker related to muscle damage and dystrophic pathology progression is matrix metalloproteinase-9 (MMP-9), a zinc- and calcium-dependent endopeptidase involved in ECM degradation and remodeling which is deregulated in DMD patients[48,49]. In a recent study, we found that *mdx* mice have a significantly higher plasma MMP-9 than wt ones, with chronic exercise further increasing its level of about 20%[15]. As shown in Figure 7B, the difference between genotypes was presently confirmed. The treatment with metformin induced a trend toward reduction of MMP-9 in chronically-exercised *mdx* mice, with a recovery score of 43%.

In dystrophic mice, the high plasma levels of the enzymes CK and LDH are well known indices of sarcolemmal fragility and metabolic sufferance, respectively. Although CK and LDH are presently not considered completely reliable biomarkers of therapeutic efficacy due to their high inter-individual sample variability and to their sensitivity to several conditions (e.g. muscle mass, activity and metabolism), metformin showed the ability to

induce a trend toward reduction for both CK and LDH in exercised *mdx* mice, with a recovery score of about 22% (Figure 7C, D).

3.4 Evaluation of metformin action on main disease-sensitive parameters in sedentary *mdx* mice

At the light of the observed results, we decided to assess the effect of long term treatment with metformin in the non-exercised *mdx* mouse model. The aim was to assess if the mechanical-metabolic sufferance associated with the protocol of chronic exercise could have limited the ability of metformin to exert its protective effects. The overall profile of metformin actions was similar, although even less important, to that observed in exercised *mdx* mice. In particular, in vivo, the treatment with metformin did not induce any significant modification on body weight of sedentary *mdx* mice and only slightly increased forelimb force (Figure 8), with no amelioration of exercise performance (data not shown). Ex vivo, metformin slightly ameliorated both twitch and tetanic tension of DIA in sedentary *mdx* mice with respect to untreated ones (sPtw: 18.2 ± 0.8 vs 15.6 ± 1.2, sP0: 85.3 ± 2.9 vs 71.4 ± 3.8; n = 7 - 8), with a recovery score of about 28% for both parameters, resulting then slightly less effective than in DIA of exercised mice. No amelioration of the same indices was observed in EDL muscle (data not shown). In line with our previous results[15], sedentary *mdx* mice showed an increased pAMPK/AMPK ratio compared to wt mice, with a higher basal level than exercised *mdx* counterparts. Similarly to exercised animals, in sedentary *mdx* mice the treatment with metformin induced a further slight increase (+8.8%) in the pAMPK/AMPK ratio, which resulted significantly different with respect to wt mice (Figure 9). In parallel, the expression pattern and level of most genes overlapped the results obtained in exercised mice, with the exception of Utrn expression, which tended to be reduced after the pharmacological

treatment (1.86 ± 0.17 vs 2.84 ± 0.82; n = 4 - 5) and of DRP1 transcript which appeared to be slightly increased by metformin (1.56 ± 0.14 vs 1 ± 0.09; n = 4 - 5). The histology profile of GC muscles from sedentary *mdx* mice showed that metformin reduced, although not significantly the total area of damage (9.4 ± 2, n = 7 vs 12.2 ± 2.3, n = 12). No significant differences in the percentage of centronucleated myofibers was found between treated and untreated mice (data not shown), while a significant increase in regenerating fibers was observed in metformin-treated animals (5.7 ± 2.1, n = 7 vs 0.7 ± 0.5, n = 12, $p < 0.01$ by Student's t test). The results of the histochemical assay for SDH in TA muscles from sedentary *mdx* mice were overlapping to those obtained in exercised ones (see Figure 6D), with no significant variation in fiber type composition induced by metformin (data not shown). The pharmacological treatment was able to induce a slight reduction of high plasma levels of LDH (1466 ± 201 vs 2834 ± 516 U/L; n = 7-8, r.s. 56%), but not of CK (5604 ± 1571 vs 4004 ± 763 U/L; n = 7-8).

3.5 Effect of metformin on muscular levels of citrulline, arginine and taurine

We investigated if our chronic treatment with metformin was able to impact on the level of amino acids known to play a role in metabolism, by assessing the concentrations of two NO precursors, L-citrulline and L-arginine, in TA muscles via HPLC. In parallel, we measured the muscular levels of taurine, an amino acid involved in many physiological processes, including metabolic response to exercise, known to be severely depleted in dystrophic muscles[50]. The results for *mdx* groups, both sedentary and exercised, are shown in Figure 10. Wt mice showed significantly higher concentrations for each amino acid with respect to *mdx* animals at all experimental conditions (citrulline: 0.044 ± 0.004, arginine: 0.34 ± 0.046, taurine 27.2 ± 5.4 µmol/mg; n = 5). L-citrulline was significantly increased by metformin in sedentary *mdx* mice, although the recovery score was modest

(13% toward wt value); this effect was less evident in exercised counterparts. A trend toward increase was observed for L-arginine in exercised treated mice with respect to the other groups (Figure 10B). Taurine levels were significantly higher in exercised *mdx* mice, although they were slightly reduced by metformin treatment with respect to their untreated control (Figure 10C).

3.6 Effect of metformin on organ weights and plasma glucose concentration

To exclude that modest efficacy could be related to any gross toxic effect due to 200 mg/kg metformin administration, the masses of vital organs (liver, heart, kidney, spleen) were measured and normalized to the body weight of each mouse. As shown in Table 2, no significant differences in organ weights were observed among all the experimental groups, except for heart weight of metformin-treated exercised *mdx* mice, which was significantly lower than in untreated controls.

In relation to the insulin-sensitizing and anti-hyperglycaemic properties of metformin[24], we also wanted to investigate how the chronic treatment with the biguanide would have impacted on glucose homeostasis in either sedentary or exercised *mdx* mice, by measuring the levels of plasma glucose by spectrophotometry. As shown in Table 2, no significant percentage variations in plasma glucose levels, calculated with respect to wt mice, were found in *mdx* experimental groups.

4. Discussion

In the past few years, the pharmacological stimulation of AMP-activated protein kinase (AMPK) via metabolic enhancers has emerged as a potential therapeutic strategy for the treatment of Duchenne muscular dystrophy (DMD)[21-23]. In the present study, we focused

on metformin, a biguanide which acts as an indirect activator of AMPK, with a long-standing evidence base for efficacy and safety as front-line treatment for type 2 diabetes[24,25]. After decades of wide clinical use, metformin has been tested as insulin-sensitizer in children and adolescents with neurogenic defects or muscle disorders, including a group of deflazacort-treated DMD boys, reducing weight gain and visceral adiposity[26]. More recently, the drug has been proposed in clinical trials on DMD patients to evaluate a potential synergistic action between AMPK and NO stimulating pathways, to improve skeletal muscle metabolism[27,28]. The pilot study (NCT02516085) revealed a positive effect of metformin in combination with L-arginine on the expression of mitochondrial proteins in vitro and in vivo, in parallel slowing the progression of disease in DMD patients between 7 and 10 years of age[27]. Despite these important results, preclinical data supporting the rationale of the use of metformin in dystrophic subjects are still poor and many aspects lead to question abouts its potential efficacy in dystrophic muscle in either murine models and DMD patients. In fact, as anticipated, the positive effects of metformin described by Ljubicic et al. refer to a short term study carried on sedentary *mdx* mice[30], which already show a basal overexpression of transcripts from protective metabolic pathways[14]. In addition, the role of metformin in the regulation of skeletal muscle metabolism and in the molecular mechanisms behind its cellular actions is controversial. A number of preclinical studies have reported that metformin primarily acts by inhibiting complex I of mitochondrial respiratory chain, leading to an increased AMP/ATP and/or ADP/ATP ratio. In turn, this enhances AMPK activation which positively regulates mitochondrial biogenesis and function[25,51]. On the other hand, metformin has also been described to improve mitochondrial respiration in murine skeletal muscle in an AMPK-independent manner, while a paradoxical dose-dependent impairment of mitochondrial function has been reported in skeletal muscle of both healthy

and diabetic rats after metformin treatment[52,53]. Importantly, *mdx* mice show defects in mitochondrial localization and ATP synthesis, which can be related to an exercise-sensitive insufficiency of complex I and complex III, while sufferance of mitochondrial respiratory chain has also been descibed in DMD patients[16,31,32,54]. In order to gain more insight into the drug mechanism of action and its efficacy in a more severe metabolic condition, as that observed in DMD patients, we performed the first in vivo and ex vivo preclinical evaluation of a long-term (20-week) treatment with metformin (200mg/kg, in drinking water) in the exercised *mdx* mouse. This model is characterized by a severe mechanical-metabolic uncoupling and functional maladaptation and we have recently found that exercise damage is associated with an altered expression of genes that are pivotal to control metabolic muscle adaptation to exercise and to counteract the action of damaging signaling pathways[14-16].

At functional level, metformin exerted modest beneficial effect on animal force and performance, being however well tollerated over the long period. Since the measure of in vivo mouse force is partially influenced by the concerted function of nervous and vascular systems, as well as by animal behavior, we assessed the muscle-specific effects of the drug on ex vivo muscle contractile parameters. Diaphragm (DIA) was chosen as a paradigm of highly compromised respiratory muscle, closely resembling disease progression in boys with Duchenne[2,55], while EDL was chosen since fast twitch limb muscles are those mainly affected by DMD[6,9]. Interestingly, we found a significant amelioration of isometric twitch and tetanic force values of isolated DIA from metformin-treated animals. This result should be taken into account for a potential therapeutic outcome, since cardiorespiratory failure represents the main cause of death in DMD patients around 20-30 years of age[2,6,34]. In contrast, there was no improvement in isometric or eccentric contraction parameters of isolated EDL muscle in response to the

treatment protocol. This discrepancy could be possibly related to an intrinsic greater susceptibility of respiratory muscles contractility to metformin action, compared to limb muscles. In a streptozotocin-induced diabetic rat model, metformin has been in fact reported to prevent the decrease of isometric contraction indices of DIA, but not of hind limb muscles (EDL and soleus)[56,57]. EDL muscle was partially protected by the treatment with respect to mechanical threshold (MT), an electrophysiological index of excitation-contraction coupling and integrated measure of calcium handling, indicating that metformin may be involved in the reduction of at least some indices of myofiber calcium-related distress, through still unclear mechanisms[9,13].

In parallel, we found that the long-term metformin administration exerted a significant protection on exercised *mdx* mice skeletal muscles from structural damage. Our histological analysis revealed that the drug markedly ameliorated several dystropathology signs in GC muscle, significantly reducing the percentage of the total area of damage (inflammatory infiltrates, non-muscular and necrotic tissue), as well as specifically of non-muscle area, which represents the portion of muscle tissue progressively replaced by fibrotic and adipose tissue, consequently to the failure of regeneration after repeated degenerative/regenerative processes in dystrophin-deficient *mdx* myofibers[6]. Importantly, we disclosed for the first time that metformin was able to significantly reduce TGF-β1 levels in dystrophic muscles, which positively correlated with histopathology results. Interestingly, our findings add novel evidences to the ability of metformin to control TGF-β1-mediated fibrosis. Such a mechanism has been described to occur directly or via inhibition of Smad-signalling, in organs and tissues from several experimental mouse models, including heart, liver and renal fibrosis[58-60]. Furthermore, metformin has been shown to attenuate TGF-β-mediated oncogenesis in various cell lines and to damper Smad2/3 activation of inhibiting mTOR/p70s6k signalling[61,62]. Thus, the present results

support a key role of metformin in controlling TGF-β-mediated fibrotic signalling also in dystrophic *mdx* muscle; considering the pivotal role of fibrosis in DMD pathology progression, the molecular mechanism underlying this action deserves more dedicated investigations for its clinical implications. The amelioration of fibrosis and the reduction of TGF-β1 induced by metformin were accompanied by a marked decrease of the levels of matrix metalloproteinase-9 (MMP-9) in plasma samples from exercised *mdx* mice. MMP-9 is an endopeptidase involved in remodeling of extracellular matrix, sarcolemmal stability and a biomarker for monitoring disease progression, which is also known to be an activator of latent TGF-β1 in skeletal muscle. This suggests a direct involvement in control of *mdx* muscle fibrosis progression[48,49,63].

Importantly, the positive effect of metformin on these key aspects of dystrophic pathology was not paralleled by any significant improvement of indices correlated to skeletal muscle metabolism. In fact, treated animals showed only a modest increase of pAMPK/AMPK ratio, measured by western blot in TA muscles, indicating a minimal level of activation of the main metabolic target of metformin. By the way, the basal higher pAMPK/AMPK can be *per se* an index of the sufferance of mitochondrial complex I[16,31,32]. In parallel, metformin only slightly modulated the transcript levels of protective genes mediating functional and metabolic adaptation of muscles to physical activity, as well as of those essential for mitochondrial biogenesis, oxidative metabolism and mitochondrial fission such as citrate synthase, Cox4 and DRP1. Also, genes involved in oxidative stress and autophagy (c-Src TK, Bnip3, Lc3), typically deregulated in dystrophic mice and targets of metformin in other disease models, such as lung adenocarcinoma, were not significantly modified[14,64,65]. In line with the lack of a main metabolic effect, metformin was unable to induce a fast-to-slow fiber type switch, as shown by SDH staining on TA muscles. We also found that the treatment only slightly reduced high plasma levels of CK and LDH,

respectively related to sarcolemmal fragility and metabolic sufferance, although the elevated inter-individual variability of these enzymes limits their reliability as biomarkers[6].

Our hypothesis that metformin could have a limited efficacy as metabolic modulator in our model, was further supported by results obtained in sedentary *mdx* mice, characterized by a milder phenotype.

Although the intrinsic defect at respiratory chain complex I and III can account for most of the limited efficacy of metformin as metabolic enhancer, other features of dystrophic muscle can also play a role.

In particular, we found that *mdx* mice, either exercised or not, had a significantly reduced muscle content of NO precursors, L-arginine and L-citrulline (synthetized from L-arginine), compared to wt and that metformin only slightly increased intracellular levels of these amino acids. In skeletal muscle, AMPK activation and NO synthesis are synergistically involved in the stimulation of mitochondrial function and biogenesis. In fact, neuronal nitric oxide synthase (nNOS), activated via AMPK, converts L-arginine in NO, in turn stimulating the AMPK – SIRT1 – PGC-1α axis[66]. The present observation discloses another key point of inadequate response of dystrophic muscle to metabolic action of metformin and provides the molecular basis in support of the therapeutic regimen combining metformin with NO precursors, proposed in DMD boys with L-arginine (NCT02516085) and with L-citrulline in a Phase III trial (NCT01995032)[27,28,67].

This is further supported by the evidences of the beneficial effects on *mdx* phenotype exerted by the admistration of L-arginine alone or in association with other therapeutics[68,69].

In addition, we found that metformin did not rescue *mdx* muscles from typical deficiency of taurine, a sulfur-containing amino acid, important for skeletal muscle function and

response to exercise[50]. Importantly, taurine is also a constituent of mitochondrial tRNAs, and the lack of taurine modification in mtRNAs has been recently reported to be responsible for respiratory chain defects and for activating global proteostress and mitochondrial disease[70,71]. Then, this is an alternative pathway for limited metabolic action of metformin and opens the way to a metformin-taurine association of clinical interest.

An epigenetic mechanism for the lack of metabolic action has also to be considered. In fact, AMPK is involved in the nuclear export and inhibition of HDACs, in order to allow the transcription of muscle metabolic genes[66]. A deregulation of Class I HDAC2 and dystrophin-NO signaling has been largely described in the *mdx* mouse. Again, this is in favour of the use of metformin in combination with other agents, i.e. HDAC inhibitors[72].

In conclusion, the present study showed for the first time that metformin has a limited efficacy on the amelioration of skeletal muscle metabolism in *mdx* mice, which in part we expected. This could, at least partly, explain why metformin is less effective in *mdx* mice compared to previously tested direct AMPK activators (*e.g.* AICAR)[21-23].

In parallel, we disclosed a potent and metabolism-independent anti-fibrotic action of metformin on *mdx* muscles which deserves to be further investigated and that support the interest of this safe and ready-to-use drug in synergic combination with other metabolic enhancers. The anti-fibrotic action may also account for an early effect at heart level, as documented by the reduction of heart mass observed herein, and in line with positive effects of metformin on cardiovascular system[73]. Our findings encourage the need to improve our knowledge on alternative, metabolism-independent drug mechanisms of action, aimed at better evaluating differently repurpose metformin for the treatment of DMD and further support its clinical use in combination with metabolism enhancers, such as NO precursors.

Acknowledgments

This research has been supported by PRIN-MIUR (Research Projects of National Interest – Ministry of Education, University and Research) project n◦ 20108YB5W3_004 and by The Dutch Duchenne Parent Project (DPP NL). The authors greatly thank Dr. Arcangela Giustino for helpful assistance during some of the experiments.

Conflicts of interest

The authors declare no conflict of interest.

References

1) Mendell JR, Lloyd-Puryear M. Report of MDA muscle disease symposium on newborn screening for Duchenne muscular dystrophy. Muscle Nerve 2013; 48(1): 21-6.

2) Hoffman EP, Dressman D. Molecular pathophysiology and targeted therapeutics for muscular dystrophy. Trends Pharmacol Sci 2001; 22: 465-70.

3) Yoshida M, Ozawa E. Glycoprotein complex anchoring dystrophin to sarcolemma. J Biochem. 1990;108(5): 748-52.

4) Petrof BJ, Shrager JB, Stedman HH, Kelly AM, Sweeney HL. Dystrophin protects the sarcolemma from stresses developed during muscle contraction. Proc Natl Acad Sci USA 1993; 90: 3710-14.

5) Lovering RM, Porter NC, Bloch RJ. The Muscular Dystrophies: From Genes to Therapies. Physical Therapy 2005; 85(12): 1372-88.

6) Grounds MD, Radley HG, Lynch GS, Nagaraju K, De Luca A. Towards developing standard operating procedures for pre-clinical testing in the mdx mouse model of Duchenne muscular dystrophy. Neurobiology of Disease 2008; 31: 1-19.

7) Bulfield G, Siller WG, Wight PA, Moore KJ. X chromosome-linked muscular dystrophy (mdx) in the mouse. Proc Natl Acad Sci U S A 1984; 81(4): 1189-92.

8) Granchelli JA, Pollina C, Hudecki MS. Pre-clinical screening of drugs using the mdx mouse. Neuromuscul Disord 2000; 10: 235-9.

9) De Luca A, Pierno S, Liantonio A, Cetrone M, Camerino C, Fraysse B, Mirabella M, Servidei S, Rüegg UT, Conte Camerino D. Enhanced dystrophic progression in mdx mice by exercise and beneficial effects of taurine and insulin-like growth factor-1. J Pharmacol Exp Ther 2003; 304(1): 453-63.

10) Fraysse B, Liantonio A, Cetrone M, Burdi R, Pierno S, Frigeri A, Pisoni M, Camerino C, De Luca A. The alteration of calcium homeostasis in adult dystrophic mdx muscle fibers is worsened by a chronic exercise in vivo. Neurobiol Dis 2004; 17(2): 144-54.

11) Rolland JF, De Luca A, Burdi R, Andreetta F, Confalonieri P, Conte Camerino D. Overactivity of exercise-sensitive cation channels and their impaired modulation by IGF-1 in mdx native muscle fibers: beneficial effect of pentoxifylline. Neurobiol Dis 2006; 24(3): 466-74.

12) Burdi R, Rolland JF, Fraysse B, Litvinova K, Cozzoli A, Giannuzzi V, Liantonio A, Camerino GM, Sblendorio V, Capogrosso RF, Palmieri B, Andreetta F, Confalonieri P, De Benedictis L, Montagnani M, De Luca A. Multiple pathological events in exercised dystrophic mdx mice are targeted by pentoxifylline: outcome of a large array of in vivo and ex vivo tests. J Appl Physiol 2009; 106(4): 1311-24.

13) Cozzoli A, Capogrosso RF, Sblendorio VT, Dinardo MM, Jagerschmidt C, Namour F, Camerino GM, De Luca A. GLPG0492, a novel selective androgen receptor modulator, improves muscle performance in the exercised-mdx mouse model of muscular dystrophy. Pharmacol Res 2013; 72: 9-24.

14) Camerino GM, Cannone M, Giustino A, Massari AM, Capogrosso RF, Cozzoli A, De Luca A. Gene expression in mdx mouse muscle in relation to age and exercise: aberrant mechanical-metabolic coupling and implications for pre-clinical studies in Duchenne muscular dystrophy. Hum Mol Genet 2014; 23(21): 5720-32.

15) Capogrosso RF, Mantuano P, Cozzoli A, Sanarica F, Massari AM, Conte E, Fonzino A, Giustino A, Rolland JF, Quaranta A, De Bellis M, Camerino GM, Grange RW, De Luca A. Contractile efficiency of dystrophic mdx mouse muscle: in vivo and ex vivo assessment of adaptation to exercise of functional endpoints. J Appl Physiol (1985) 2017; 122(4): 828-43.

16) Gamberi T, Fiaschi T, Valocchia E, Modesti A, Mantuano P, Rolland JF, Sanarica F, De Luca A, Magherini F. Proteome analysis in dystrophic mdx mouse muscle reveals a drastic alteration of key metabolic and contractile proteins after chronic exercise and the potential modulation by anti-oxidant compounds. J Proteomics 2018; 170: 43-58.

17) Handschin C, Kobayashi YM, Chin S, Seale P, Campbell KP, Spiegelman BM. PGC-1α regulates the neuromuscular junction program and ameliorates Duchenne muscular dystrophy. Genes Dev 2007; 21(7): 770-83.

18) Selsby JT, Morine KJ, Pendrak K, Barton ER, Sweeney HL. Rescue of dystrophic skeletal muscle by PGC-1α involves a fast to slow fiber type shift in the mdx mouse. PLoS One 2012; 7(1): e30063.

19) Hollinger K, Gardan-Salmon D, Santana C, Rice D, Snella E, Selsby JT. Rescue of dystrophic skeletal muscle by PGC-1α involves restored expression of dystrophin-associated protein complex components and satellite cell signaling. Am J Physiol Regul Integr Comp Physiol 2013; 305(1): R13-23.

20) Cantó C, Auwerx J. PGC-1alpha, SIRT1 and AMPK, an energy sensing network that controls energy expenditure. Curr Opin Lipidol 2009; 20(2): 98-105.

21) Ljubicic V, Miura P, Burt M, Boudreault L, Khogali S, Lunde JA, Renaud JM, Jasmin BJ. Chronic AMPK activation evokes the slow, oxidative myogenic program and triggers beneficial adaptations in mdx mouse skeletal muscle. Hum Mol Genet 2011; 20(17): 3478-93.

22) Jahnke VE, Van Der Meulen JH, Johnston HK, Ghimbovschi S, Partridge T, Hoffman EP, Nagaraju K. Metabolic remodeling agents show beneficial effects in the dystrophin-deficient mdx mouse model. Skelet Muscle 2012; 2(1): 16.

23) Pauly M, Daussin F, Burelle Y, Li T, Godin R, Fauconnier J, Koechlin-Ramonatxo C, Hugon G, Lacampagne A, Coisy-Quivy M, Liang F, Hussain S, Matecki S, Petrof BJ.

AMPK activation stimulates autophagy and ameliorates muscular dystrophy in the mdx mouse diaphragm. Am J Pathol 2012; 181(2): 583-92.

24) Nathan DM, Buse JB, Davidson MB, Ferrannini E, Holman RR, Sherwin R, Zinman B; American Diabetes Association; European Association for Study of Diabetes. Medical management of hyperglycemia in type 2 diabetes: a consensus algorithm for the initiation and adjustment of therapy: a consensus statement of the American Diabetes Association and the European Association for the Study of Diabetes. Diabetes Care 2009;32(1): 193-203.

25) Viollet B, Guigas B, Sanz Garcia N, Leclerc J, Foretz M, Andreelli F. Cellular and molecular mechanisms of metformin: an overview. Clin Sci (Lond) 2012; 122(6): 253-270.

26) Casteels K, Fieuws S, van Helvoirt M, Verpoorten C, Goemans N, Coudyzer W, Loeckx D, de Zegher F. Metformin therapy to reduce weight gain and visceral adiposity in children and adolescents with neurogenic or myogenic motor deficit. Pediatr Diabetes 2010; 11:61-9.

27) Hafner P, Bonati U, Erne B, Schmid M, Rubino D, Pohlman U, Peters T, Rutz E, Frank S, Neuhaus C, Deuster S, Gloor M, Bieri O, Fischmann A, Sinnreich M, Gueven N, Fischer D. Improved Muscle Function in Duchenne Muscular Dystrophy through L-Arginine and Metformin: An Investigator-Initiated, Open-Label, Single-Center, Proof-Of-Concept-Study. PLoS One 2016; 11(1): e0147634.

28) Hafner P, Bonati U, Rubino D, Gocheva V, Zumbrunn T, Gueven N, Fischer D. Treatment with L-citrulline and metformin in Duchenne muscular dystrophy: study protocol for a single-centre, randomised, placebo-controlled trial. Trials 2016;17(1):389.

29) Langone F, Cannata S, Fuoco C, Lettieri Barbato D, Testa S, Nardozza AP, Ciriolo MR, Castagnoli L, Gargioli C, Cesareni G. Metformin protects skeletal muscle from cardiotoxin induced degeneration. PLoS One 2014; 9(12): e114018.

30) Ljubicic V, Jasmin BJ. Metformin increases peroxisome proliferator-activated receptor γ Co-activator-1α and utrophin A expression in dystrophic skeletal muscle. Muscle Nerve 2015; 52(1):139-42.

31) Rybalka E, Timpani CA, Cooke MB, Williams AD, Hayes A. Defects in Mitochondrial ATP Synthesis in Dystrophin-Deficient Mdx Skeletal Muscles May Be Caused by Complex I Insufficiency. Ervasti JM, ed. PLoS ONE 2014; 9(12): e115763.

32) Timpani CA, Hayes A, Rybalka E. Revisiting the dystrophin-ATP connection: How half a century of research still implicates mitochondrial dysfunction in Duchenne Muscular Dystrophy aetiology. Med Hypotheses 2015;85(6):1021-33.

33) De Luca A, Nico B, Liantonio A, Didonna MP, Fraysse B, Pierno S, Burdi R, Mangieri D, Rolland JF, Camerino C, Zallone A, Confalonieri P, Andreetta F, Arnoldi E, Courdier-Fruh I, Magyar JP, Frigeri A, Pisoni M, Svelto M, Conte Camerino D. A multidisciplinary evaluation of the effectiveness of cyclosporine a in dystrophic mdx mice. Am J Pathol 2005; 166: 477-89.

34) Bushby K, Finkel R, Birnkrant DJ, Case LE, Clemens PR, Cripe L, Kaul A, Kinnett K, McDonald C, Pandya S, Poysky J, Shapiro F, Tomezsko J, Constantin C; DMD Care Considerations Working Group. Diagnosis and management of Duchenne muscular dystrophy, part 1: diagnosis, and pharmacological and psychosocial management. Lancet Neurol 2010; 9(1):77-93.

35) Reagan-Shaw S, Nihal M, Ahmad N. Dose translation from animal to human studies revisited. FASEB J 2008;22(3):659-61.

36) Capogrosso RF, Mantuano P, Uaesoontrachoon K, Cozzoli A, Giustino A, Dow T,Srinivassane S, Filipovic M, Bell C, Vandermeulen J, Massari AM, De Bellis M, Conte E, Pierno S, Camerino GM, Liantonio A, Nagaraju K, De Luca A. Ryanodine channel complex stabilizer compound S48168/ARM210 as a disease modifier indystrophin-deficient mdx mice: proof-of-concept study and independent validation of efficacy. FASEB J 2017;32(2):1025-1043.

37) Willmann R, De Luca A, Benatar M, Grounds, M, Dubach, J, Raymackers, J-M, Nagaraju, K. Enhancing translation: guidelines for standard pre-clinical experiments in mdx mice. Neuromuscular Disorders 2012; 22(1): 43-49.

38) Moorwood C, Liu M, Tian Z, Barton ER. Isometric and eccentric force generation assessment of skeletal muscles isolated from murine models of muscular dystrophies. J Vis Exp 2013; 71.

39) Brooks SV, Faulkner JA. Contractile properties of skeletal muscle of young, adult and aged mice. J Physiol 1988; 404: 71-82.

40) Zanou N, Iwata Y, Schakman O, Lebacq J, Wakabayashi S, Gailly P. Essential role of TRPV2 ion channel in the sensitivity of dystrophic muscle to eccentric contractions. FEBS Lett 2009; 583: 3600-3604.

41) De Luca A, Pierno S, Liantonio A, Cetrone M, Camerino C, Simonetti S, Papadia F, Conte Camerino D. Alteration of excitation-contraction coupling mechanism in extensor digitorum longus muscle fibres of dystrophic mdx mouse and potential efficacy of taurine. Br J Pharmacol 2001; 132: 1047-54.

42) Cozzoli A, Liantonio A, Conte E, Cannone M, Massari AM, Giustino A, Scaramuzzi A, Pierno S, Mantuano P, Capogrosso RF, Camerino GM, De Luca A. Angiotensin II modulates mouse skeletal muscle resting conductance to chloride and potassium ions and

calcium homeostasis via the AT1 receptor and NADPH oxidase. Am J Physiol Cell Physiol 2014; 307(7): C634-47.

43) Steinberg GR, O'Neill HM, Dzamko NL, Galic S, Naim T, Koopman R, Jørgensen SB, Honeyman J, Hewitt K, Chen ZP, Schertzer JD, Scott JW, Koentgen F, Lynch GS, Watt MJ, van Denderen BJ, Campbell DJ, Kemp BE. Whole body deletion of AMP-activated protein kinase β2 reduces muscle AMPK activity and exercise capacity. J Biol Chem 2010; 285(48):37198-209.

44) Bustin SA, Benes V, Garson JA, Hellemans J, Huggett J, et al. (2009) The MIQE guidelines: Minmum Information for publication of Quantitative real-time PCR Experiments. Clin Chem 55(4): 611-622.

45) Tucci P, Mhillaj E, Morgese MG, Colaianna M, Zotti M, Schiavone S, Cicerale M, Trezza V, Campolongo P, Cuomo V, Trabace L. Memantine prevents memory consolidation failure induced by soluble beta amyloid in rats. Frontiers in Behavioral Neuroscience 2014; 8:332.

46) De Luca A, Nico B, Rolland JF, Cozzoli A, Burdi R, Mangieri D, Giannuzzi V, Liantonio A, Cippone V, De Bellis M, Nicchia GP, Camerino GM, Frigeri A, Svelto M, Camerino DC. Gentamicin treatment in exercised mdx mice: Identification of dystrophin-sensitive pathways and evaluation of efficacy in work-loaded dystrophic muscle. Neurobiol Dis 2008; 32(2): 243-53.

47) Capogrosso RF, Cozzoli A, Mantuano P, Camerino GM, Massari AM, Sblendorio VT, De Bellis M, Tamma R, Giustino A, Nico B, Montagnani M, De Luca A. Assessment of resveratrol, apocynin and taurine on mechanical-metabolic uncoupling and oxidative stress in a mouse model of duchenne muscular dystrophy: A comparison with the gold standard, α-methyl prednisolone. Pharmacol Res 2016; 106:101-113.

48) Nadarajah VD, van Putten M, Chaouch A, Garrood P, Straub V, Lochmüller H, Ginjaar HB, Aartsma-Rus AM, van Ommen GJ, den Dunnen JT, 't Hoen PA. Serum matrix metalloproteinase-9 (MMP-9) as a biomarker for monitoring disease progression in Duchenne muscular dystrophy (DMD). Neuromuscul Disord 2011; 21(8): 569-8.

49) Ogura Y, Tajrishi MM, Hindi SM, Kumar A. Therapeutic potential of matrix metalloproteinases in Duchenne muscular dystrophy. Front Cell Dev Biol 2014; 2: 1-11.

50) De Luca A, Pierno S, Camerino DC. Taurine: the appeal of a safe amino acid for skeletal muscle disorders. J Transl Med 2015; 13:243.

51) Rena G, Pearson ER, Sakamoto K. Molecular mechanism of action of metformin: old or new insights? Diabetologia 2013; 56(9):1898-906.

52) Kristensen JM, Treebak JT, Schjerling P, Goodyear L, Wojtaszewski JF. Two weeks of metformin treatment induces AMPK-dependent enhancement of insulin-stimulated glucose uptake in mouse soleus muscle. Am J Physiol Endocrinol Metab 2014;306(10): E1099-109.

53) Wessels B, Ciapaite J, van den Broek NM, Nicolay K, Prompers JJ. Metformin impairs mitochondrial function in skeletal muscle of both lean and diabetic rats in a dose-dependent manner. PLoS One 2014;9(6):e100525.

54) Percival JM, Siegel MP, Knowels G, Marcinek DJ. Defects in mitochondrial localization and ATP synthesis in the mdx mouse model of Duchenne muscular dystrophy are not alleviated by PDE5 inhibition. Hum Mol Genet 2013; 22(1): 153-167.

55) Lynch GS, Rafael JA, Hinkle RT, Cole NM, Chamberlain JS, Faulkner JA. Contractile properties of diaphragm muscle segments from old mdx and old transgenic mdx mice. Am J Physiol 1997; 272: C2063-8.

56) McGuire M, MacDermott M. The influence of streptozotocin-induced diabetes and the antihyperglycaemic agent metformin on the contractile characteristics and the membrane potential of the rat diaphragm. Exp Physiol 1998;83(4): 481-7.

57) McGuire M, MacDermott M. The influence of streptozotocin diabetes and metformin on erythrocyte volume and on the membrane potential and the contractile characteristics of the extensor digitorum longus and soleus muscles in rats. Exp Physiol 1999;84(6):1051-8.

58) Xiao H, Ma X, Feng W, Fu Y, Lu Z, Xu M, Shen Q, Zhu Y, Zhang Y. Metformin attenuates cardiac fibrosis by inhibiting the TGFbeta1-Smad3 signalling pathway. Cardiovasc Res 2010;87(3): 504-13.

59) Fan K, Wu K, Lin L, Ge P, Dai J, He X, Hu K, Zhang L. Metformin mitigates carbon tetrachloride-induced TGF-β1/Smad3 signaling and liver fibrosis in mice. Biomed Pharmacother 2017; 90:421-426.

60) Feng Y, Wang S, Zhang Y, Xiao H. Metformin attenuates renal fibrosis in both AMPKα2-dependent and independent manners. Clin Exp Pharmacol Physiol 2017;44(6):648-655.

61) Cheng K & Hao M. Metformin Inhibits TGF-β1-Induced Epithelial-to-Mesenchymal Transition via PKM2 Relative-mTOR/p70s6k Signaling Pathway in Cervical Carcinoma Cells. Int J Mol Sci 2016;17(12).

62) Wahdan-Alaswad R, Harrell JC, Fan Z, Edgerton SM, Liu B, Thor AD. Metformin attenuates transforming growth factor beta (TGF-β) mediated oncogenesis in mesenchymal stem-like/claudin-low triple negative breast cancer. Cell Cycle 2016;15(8):1046-59.

63) Shiba N, Miyazaki D, Yoshizawa T, Fukushima K, Shiba Y, Inaba Y, Imamura M, Takeda S, Koike K, Nakamura A. Differential roles of MMP-9 in early and late stages of dystrophic muscles in a mouse model of Duchenne muscular dystrophy. Biochim Biophys Acta 2015; 1852(10 Pt A): 2170-2182.

64) Pal R, Palmieri M, Loehr JA, Li S, Abo-Zahrah R, Monroe TO, Thakur PB, Sardiello M, Rodney GG. Src-dependent impairment of autophagy by oxidative stress in a mouse model of Duchenne muscular dystrophy. Nat Commun 2014; 5:4425.

65) Nazim UM, Moon JH, Lee JH, Lee YJ, Seol JW, Eo SK, Lee JH, Park SY. Activation of autophagy flux by metformin downregulates cellular FLICE-like inhibitory protein and enhances TRAIL- induced apoptosis. Oncotarget 2016; 7(17):23468-81.

66) McGee SL, Hargreaves M. Histone modifications and skeletal muscle metabolic gene expression. Clin Exp Pharmacol Physiol 2010;37(3):392-6.

67) Wijnands KA, Vink H, Briedé JJ, van Faassen EE, Lamers WH, Buurman WA, Poeze M. Citrulline a more suitable substrate than arginine to restore NO production and the microcirculation during endotoxemia. PLoS One 2012; 7(5): e37439.

68) Voisin V, Sébrié C, Matecki S, Yu H, Gillet B, Ramonatxo M, Israël M, de la Porte S. L-arginine improves dystrophic phenotype in mdx mice. Neurobiol Dis 2005;20(1):123-30.

69) Vianello S, Yu H, Voisin V, Haddad H, He X, Foutz AS, Sebrié C, Gillet B,Roulot M, Fougerousse F, Perronnet C, Vaillend C, Matecki S, Escolar D, Bossi L, Israël M, de la Porte S. Arginine butyrate: a therapeutic candidate for Duchenne muscular dystrophy. FASEB J 2013;27(6): 2256-69.

70) Suzuki T, Nagao A, Suzuki T. Human mitochondrial diseases caused by lack of taurine modification in mitochondrial tRNAs. Wiley Interdiscip Rev RNA. 2011;2:376–386.

71) Fakruddin M, Wei FY, Suzuki T, Asano K, Kaieda T, Omori A, Izumi R, Fujimura A, Kaitsuka T, Miyata K, Araki K, Oike Y, Scorrano L, Suzuki T, Tomizawa K. Defective Mitochondrial tRNA Taurine Modification Activates Global Proteostress and Leads to Mitochondrial Disease. Cell Rep 2018;22(2): 482-496.

72) Consalvi S, Mozzetta C, Bettica P, Germani M, Fiorentini F, Del Bene F, Rocchetti M, Leoni F, Monzani V, Mascagni P, Puri PL, Saccone V. Preclinical studies in the mdx

mouse model of duchenne muscular dystrophy with the histone deacetylase inhibitor givinostat. Mol Med 2013; 20(19):79-87.

73) Nesti L, Natali A. Metformin effects on the heart and the cardiovascular system: A review of experimental and clinical data. Nutr Metab Cardiovasc Dis 2017;27(8):657-669.

Figure Legends

Figure 1: In vivo efficacy of metformin in exercised *mdx* mice. Each graph shows the variations in body weight (A), forelimb grip strength (B) and grip strength normalized on body weight (C) at the beginning of the treatment protocol (T0) and after 8 (T8), 12 (T12), 16 (T16) and 20 (T20) weeks for wild type (wt) and treated/untreated exercised *mdx* mice. All values are expressed as means ± SEM from the number of mice indicated in brackets. In A, a significant difference among groups was found by ANOVA analysis at time points T0, T8, T12 and T16, with $F > 4.04$, $p < 0.04$. Bonferroni post hoc for individual differences between groups are as follows: significantly different vs *wt mice ($p < 0.007$). In B, a significant difference among groups was found by ANOVA analysis at all the time points, with $F > 6.91$, $p < 0.007$. Bonferroni post hoc for individual differences between groups are as follows: significantly different vs *wt mice (4.29×10^{-5} $p < 0.006$). In C, a significant difference among groups was found by ANOVA analysis at all the time points, with $F > 16.16$, $p < 0.0001$. Bonferroni post hoc for individual differences between groups are as follows: significantly different vs. *wt mice ($1.51 \times 10^{-6} < p < 0.005$); °vehicle-treated *mdx* mice ($p < 0.008$).

Figure 2: Effects of metformin on ex vivo force of isolated muscles. In A and B are shown the normalized values of maximal isometric twitch (*A*, sPtw measured in kN/m^2) and tetanic (*B*, sP0 measured in kN/m^2) tensions of diaphragm strips from wt and treated/untreated exercised *mdx* mice. In C and D are shown the normalized values of sPtw (C) and sP0 (D) for EDL muscle from the same experimental groups. Each value is expressed as the mean ± SEM from the number of mice indicated in brackets. For diaphragm, a significant difference among groups was found by ANOVA analysis ($F > 7.86$, $p < 0.005$). Bonferroni post hoc for

individual differences between groups are as follows: significantly different vs * wt mice ($p < 0.001$); ° vs mdx exer ($p < 0.003$). For EDL muscle, a significant difference among groups was found by ANOVA analysis ($F > 13.36$, $p < 0.0008$). Bonferroni post hoc for individual differences between groups are as follows: significantly different vs * wt mice ($p < 0.0005$).

Figure 3: Effect of treatment on the voltage threshold for contraction of EDL muscle fibers. The figure shows the strength-duration curves with the values of voltage threshold for contraction at increasing pulse durations (mechanical threshold) of EDL myofibers from wt and treated/untreated exercised *mdx* mice. Each value is expressed as the mean ± S.E.M. from 6-33 fibers sampled from 3-4 preparations. A significant difference among groups was found by ANOVA analysis for voltage threshold values at 500 ms ($F > 31.3$; $p < 3 \times 10^{-10}$) 200 ms ($F > 20$; $p < 2.8 \times 10^{-7}$) 100 ms ($F > 28.9$; $p < 1.8 \times 10^{-9}$), 50 ms ($F > 46.5$; $p < 2.6 \times 10^{-12}$), 20 ms ($F > 10.9$; $p < 0.0002$) and 10 ms ($F > 5.31$; $p < 0.01$) pulse durations. Bonferroni post hoc correction is as follows: Significantly different * vs wt ($4.7 \times 10^{-5} < p < 5 \times 10^{-13}$); ° vs exercised *mdx* + vehicle ($0.006 < p < 5.6 \times 10^{-7}$).

Figure 4: Effect of metformin on phosphorylated AMPK/AMPK ratio. In A are shown representative western blots of total AMPK and phosphorylated AMPK (pAMPK) in TA muscles from wt and treated/untreated exercised *mdx* mice. In B, a box plot with whiskers indicating the minimum to maximum range, illustrates the distribution of individual data points (grey dots) for pAMPK/AMPK ratio in the experimental groups. In C is shown the calculation of pAMPK/AMPK ratio; each value is expressed as the mean ± SEM from the number of mice indicated in brackets. No significant differences were found by ANOVA + Bonferroni post hoc. *A significant difference of metformin-treated *mdx* mice vs wt ($p < 0.05$) was found by unpaired Student's t test.

Figure 5: Modulation of gene expression by metformin treatment. The figure shows the transcriptional levels measured by qPCR, of exercise-sensitive genes related to AMPK activation (PGC-1α, SIRT1, PPARγ e PPARβ/δ, utrophin, Src-TK), genes involved in mitochondrial function and metabolism (DRP1, Cs, Cox4) and autophagy genes (Bnip3, Lc3), in GC muscles from treated and untreated exercised *mdx* mice. Each bar is the mean ± SEM from the number of mice indicated in brackets. Transcript levels were normalized on the housekeeping gene GAPDH. No statistically significant differences were found by unpaired Student's t test.

Figure 6: Effect of metformin on muscle histology profile. In A are shown representative sections of hematoxylin & eosin-stained GC muscles from treated and untreated exercised *mdx* mice (10X magnification), both characterized by a disorganized tissue architecture with the presence of centronucleated fibers, inflammatory infiltrates and areas of non-muscle tissue, typical signs of dystrophic histopathology. In B is shown the calculated percentage of both total area of damage and non-muscle area in GC muscles from wt and exercised *mdx* mice groups. Each bar is the mean ± SEM from at least 5 muscles and 3 fields for each muscle preparation. A significant difference among groups was found by ANOVA analysis ($F > 9.4$, $p < 0.002$). Bonferroni post hoc for individual differences between groups are as follows: significantly different vs *wt mice ($p < 0.0007$), °vehicle-treated *mdx* mice ($p < 0.001$). For total damage, a significant difference for metformin-treated *mdx* mice vs wt (§, $p < 0.03$) was found by unpaired Student's t test. In C are shown representative sections of SDH-stained TA muscles from treated/untreated exercised *mdx* mice. SDH stain allows to distinguish between oxidative (darker) and less oxidative/non-oxidative myofibers in both

sections. The quantitative analysis (D) did not reveal any statistically significant variation among the treatment groups.

Figure 7: Effect of metformin on biomarkers of muscle damage. In A are shown the levels of pro-fibrotic TGF-β1 marker normalized on total protein content (pg/μg) measured in GC muscles samples from wt and treated/untreated *mdx* mice by ELISA. The statistical analysis by ANOVA found a significant difference among groups ($F = 6.08$, $p < 0.02$). Significant differences between single groups were found by unpaired Student's t test: vs *wt mice ($p < 0.05$); §*mdx* mice treated with vehicle ($p < 0.02$). In B are shown the plasma levels of matrix metalloproteinase-9 (MMP-9) measured by ELISA in the different experimental groups. A significant difference among groups was found by ANOVA analysis ($F= 7.28$ $p < 0.008$). Bonferroni post hoc for individual differences between groups are as follows: significantly different vs *wt mice ($p < 0.002$). In C and D are shown the levels of creatine kinase and lactate dehydrogenase measured in plasma samples from the different experimental groups by spectrophotometry. A significant difference among groups was found by ANOVA analysis ($F > 4.01$, $p < 0.04$). Bonferroni post hoc for individual differences between groups are as follows: significantly different vs * wt mice ($p < 0.003$). All values are expressed as means ± SEM from the number of mice indicated in brackets.

Figure 8: Effects of metformin on in vivo parameters in sedentary *mdx* mice. Each graph shows the variations in body weight (A), forelimb grip strength (B) and forelimb grip strength normalized on body weight (C) at the beginning of the treatment protocol (T0) and after 8 (T8), 12 (T12), 16 (T16) and 20 (T20) weeks for wild type (wt) and treated/untreated sedentary *mdx* mice. All values are expressed as means ± SEM from the number of mice indicated in brackets. In A, a significant difference among groups was found by ANOVA

analysis at time points from T8 to T20, with $F > 4.13$, $p < 0.04$. Bonferroni post hoc for individual differences between groups are as follows: significantly different vs *wt mice ($6.17 \times 10^{-6} < p < 0.002$). In B, a significant difference among groups was found by ANOVA analysis at time points T0, T12, T16 and T20 ($F > 3.08$, $p < 0.05$). Bonferroni post hoc for individual differences between groups are as follows: significantly different vs *wt mice (4.3×10^{-7} $p < 0.007$). In C, a significant difference among groups was found by ANOVA analysis at all the time points, with $F > 3.31$, $p < 0.04$. Bonferroni post hoc for individual differences between groups are as follows: significantly different vs. *wt mice ($1.06 \times 10^{-7} < p < 0.005$).

Figure 9: Effect of metformin on phosphorylated AMPK/AMPK ratio in sedentary *mdx* mice. In A are shown representative western blots of total AMPK and phosphorylated AMPK (pAMPK) in TA muscles from wt and treated/untreated sedentary *mdx* mice. In B, a box plot with whiskers indicating the minimum to maximum range, illustrates the distribution of individual data points (grey dots) for pAMPK/AMPK ratio in the experimental groups. In C is shown the calculation of pAMPK/AMPK ratio; each value is expressed as the mean ± SEM from the number of mice indicated in brackets. A significant difference among groups was found by ANOVA analysis ($F > 3.73$, $p < 0.04$). Bonferroni post hoc for individual differences between groups are as follows: significantly different vs *wt ($p < 0.006$).

Figure 10: Effect of metformin on muscular levels of citrulline, arginine and taurine. Concentrations of the amino acids L-citrulline (A), L-arginine (B) and taurine (C) in tibialis anterior muscles from non-exercised/exercised mdx mice, treated or not with metformin. Each value is expressed as the mean ± SEM from 5-7 animals. In A and C, a significant difference among groups were found by ANOVA analysis followed by Bonferroni post hoc correction (* $p < 0.05$; *** $p < 0.0001$).

Figure 1

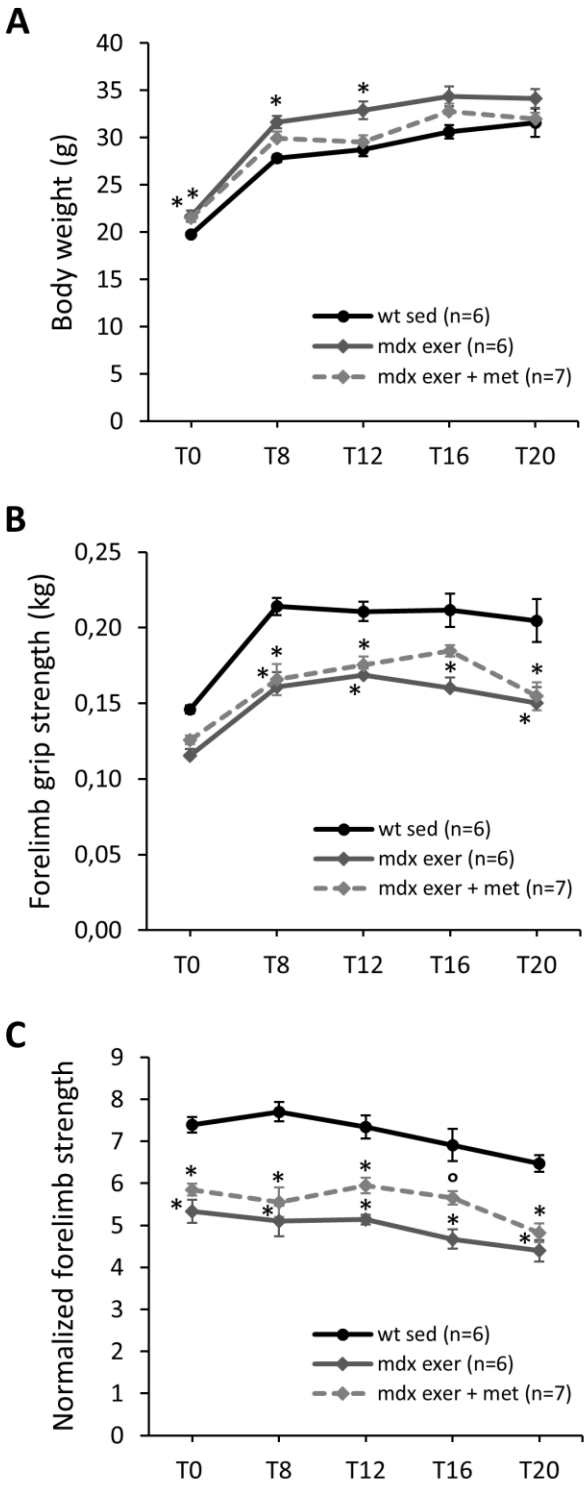

Figure 2

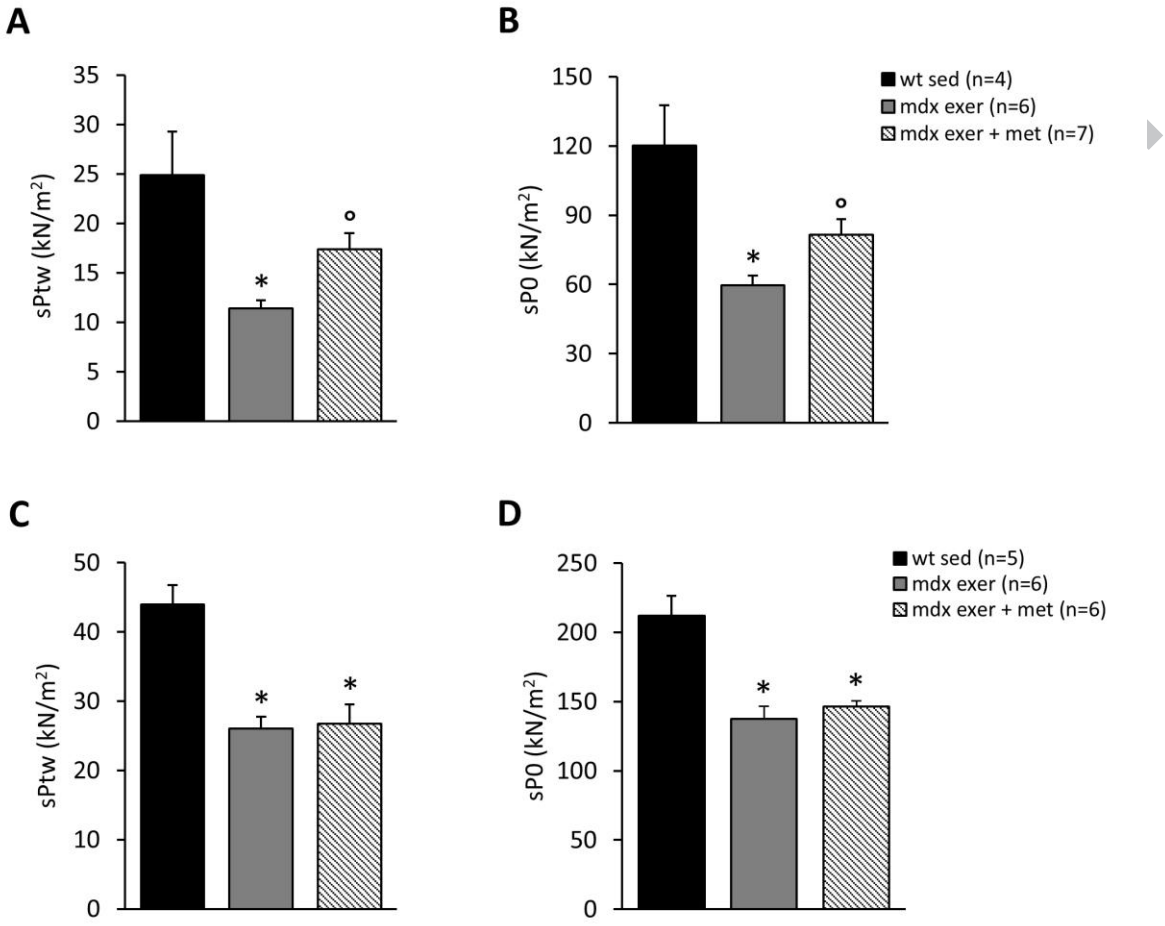
A
B
C
D
sPtw (kN/m²)
sP0 (kN/m²)
wt sed (n=4)
mdx exer (n=6)
mdx exer + met (n=7)
wt sed (n=5)
mdx exer (n=6)
mdx exer + met (n=6)
*
°

Figure 3

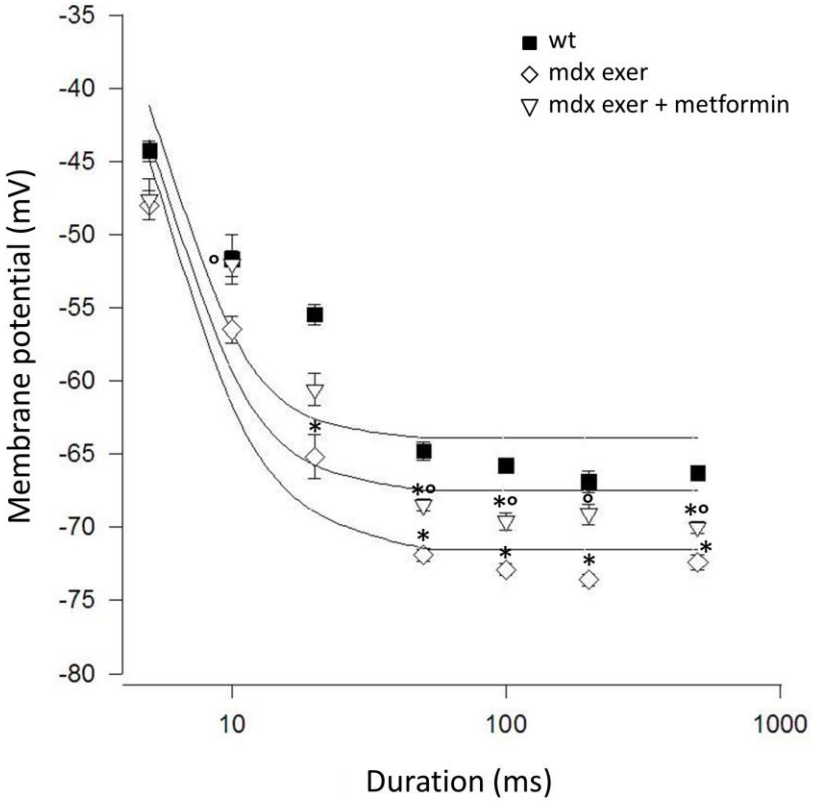

Figure 4

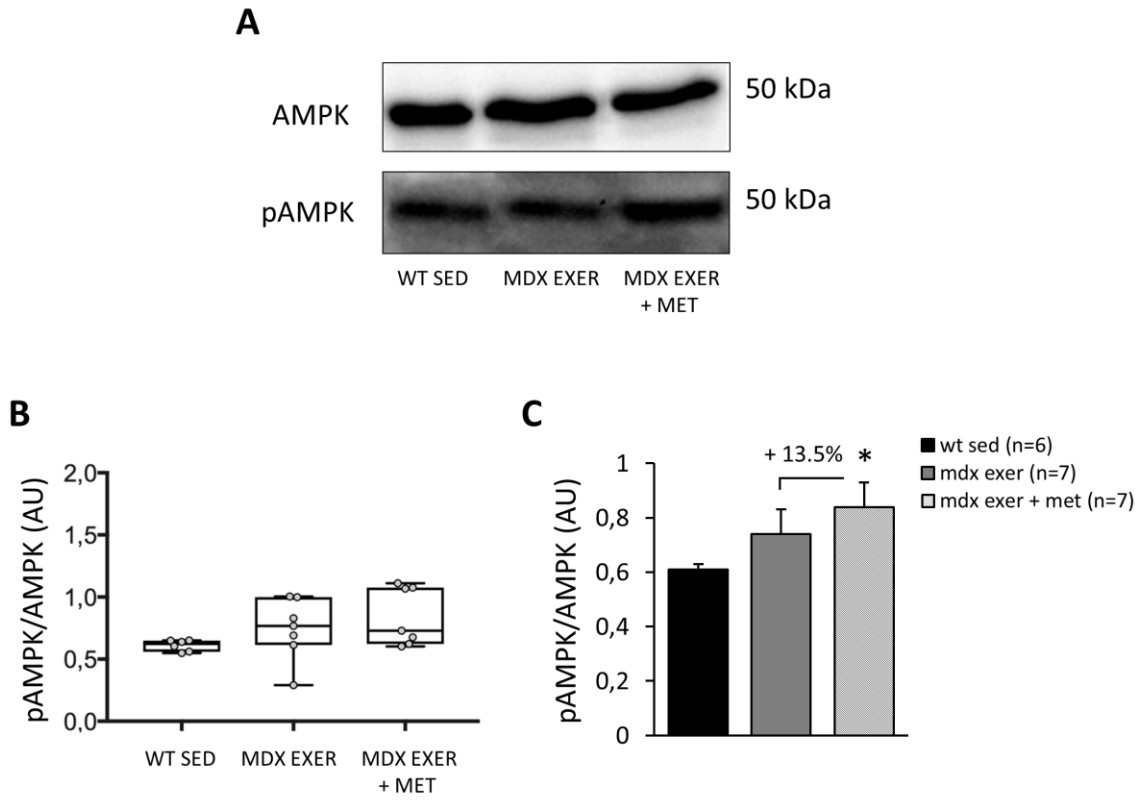

Figure 5

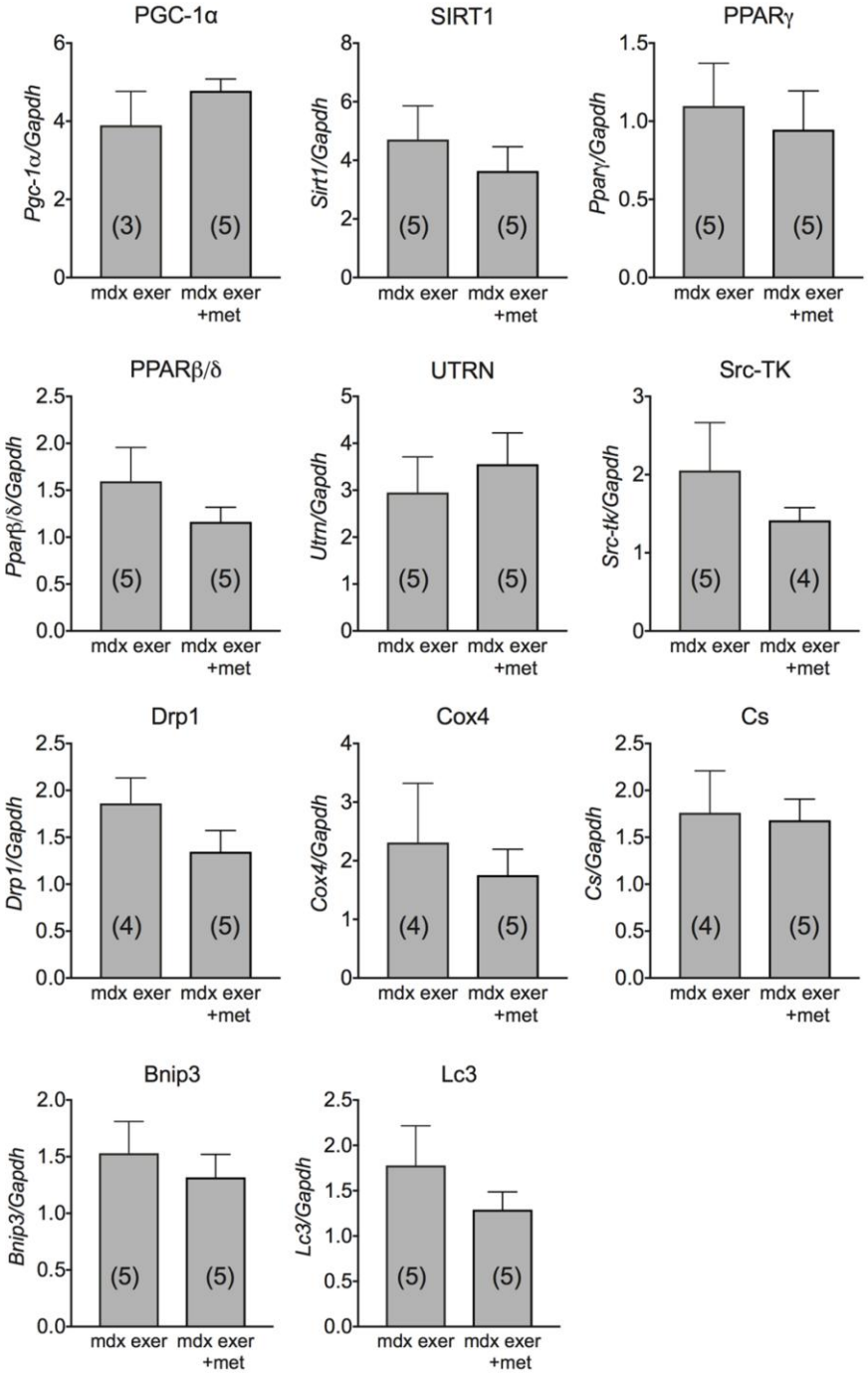

Figure 6

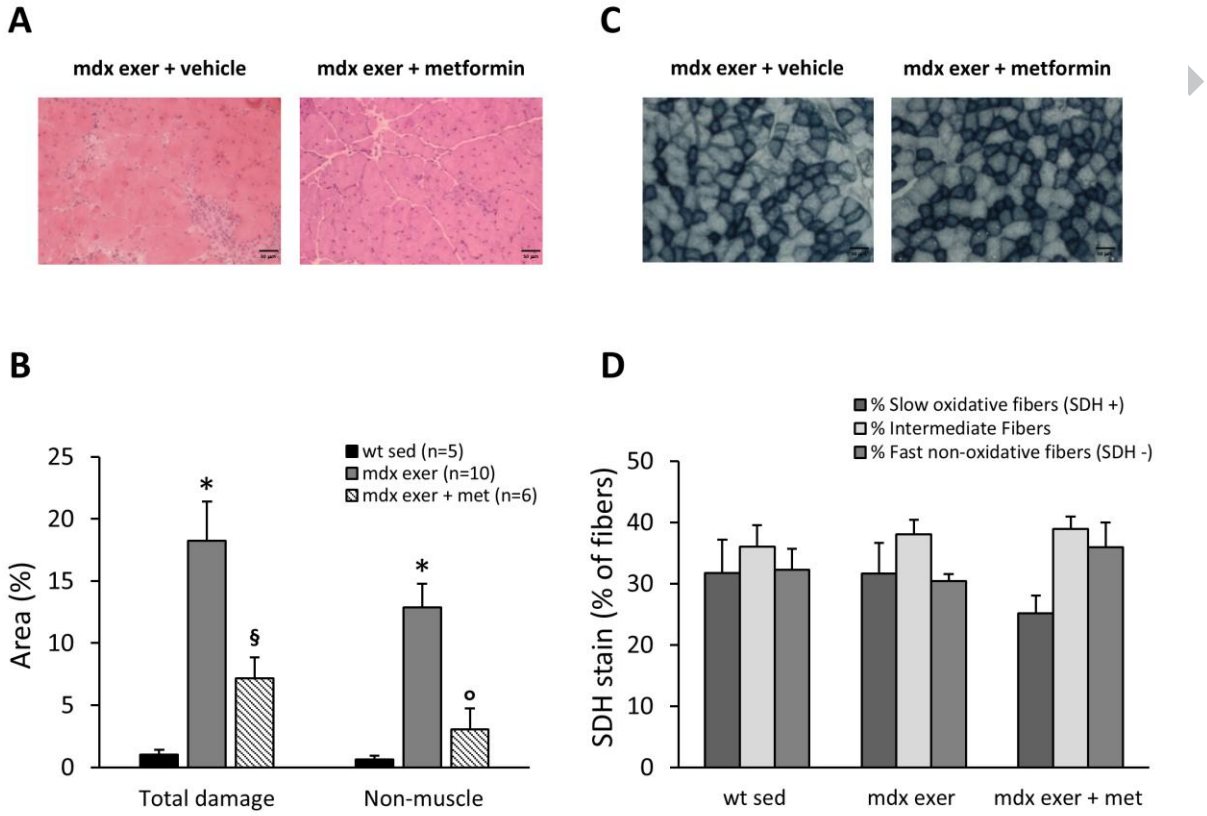

Figure 7

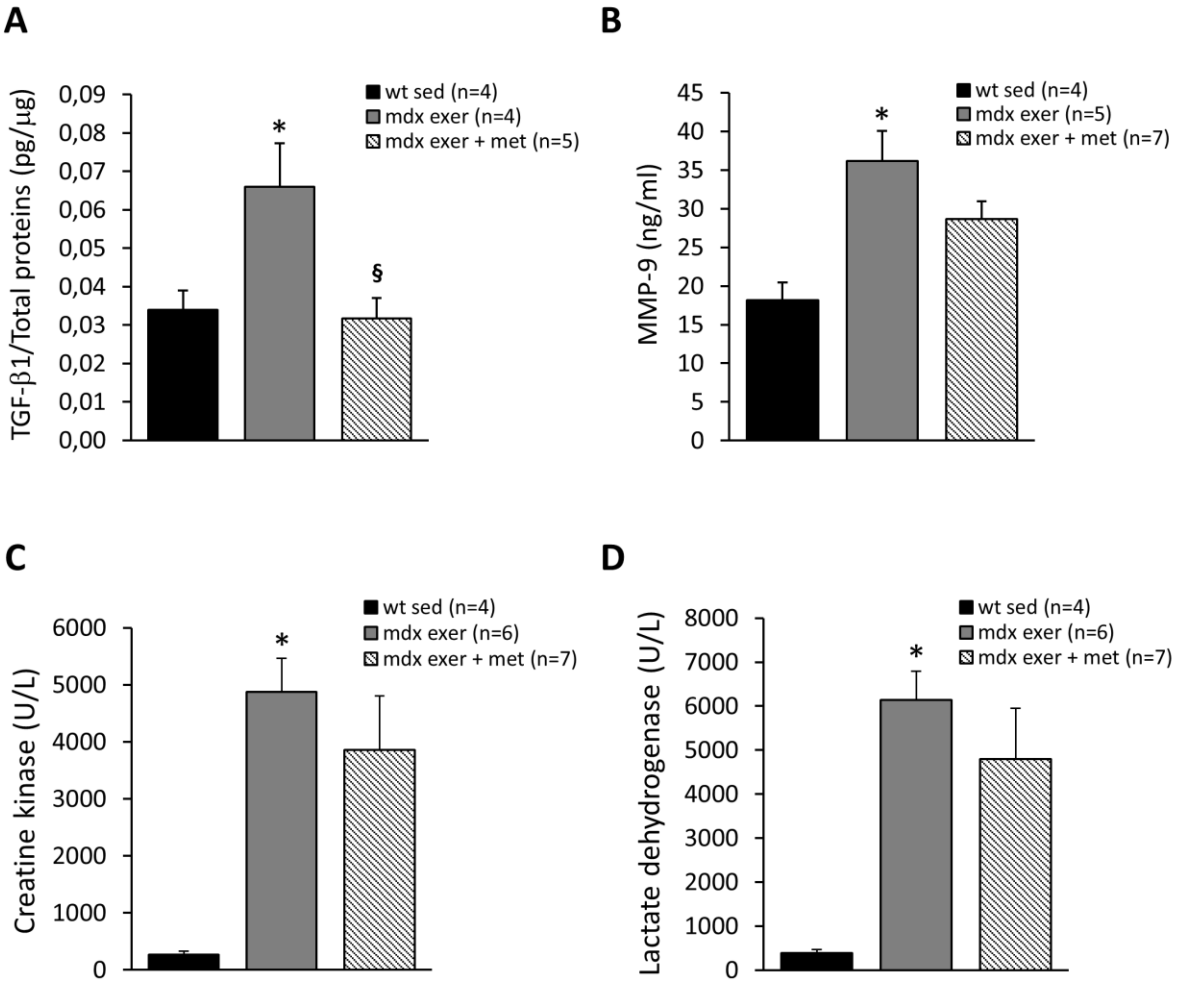

Figure 8

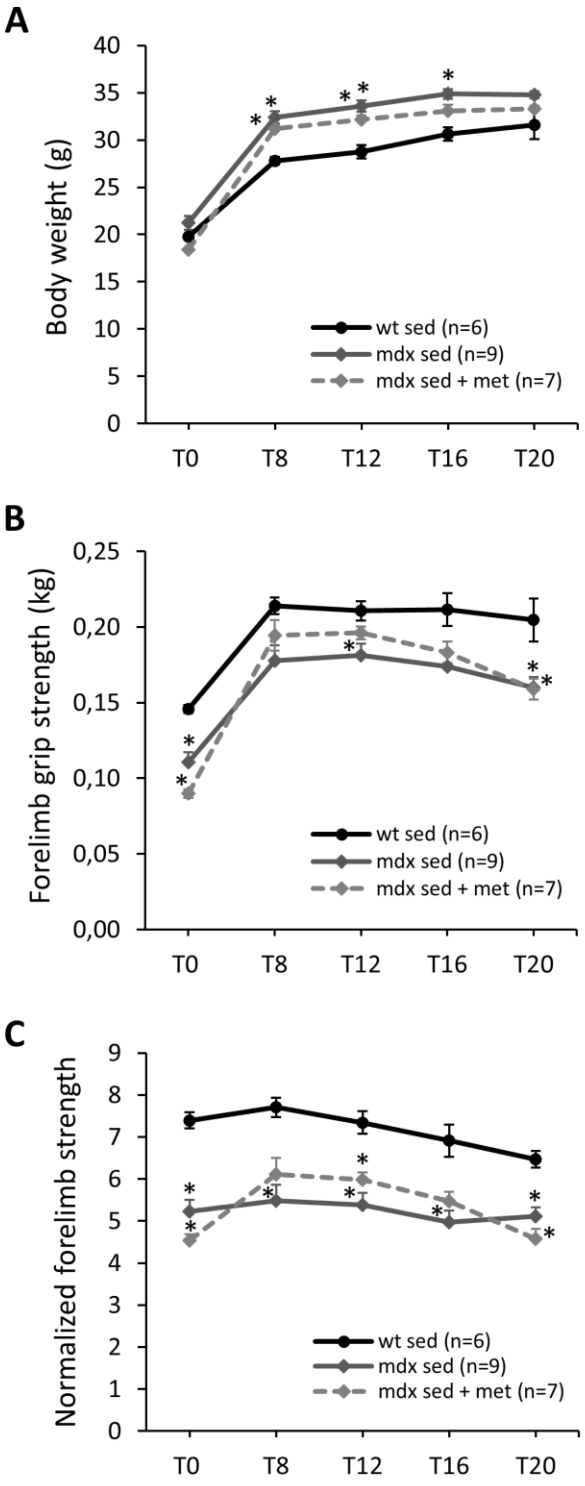

Figure 9

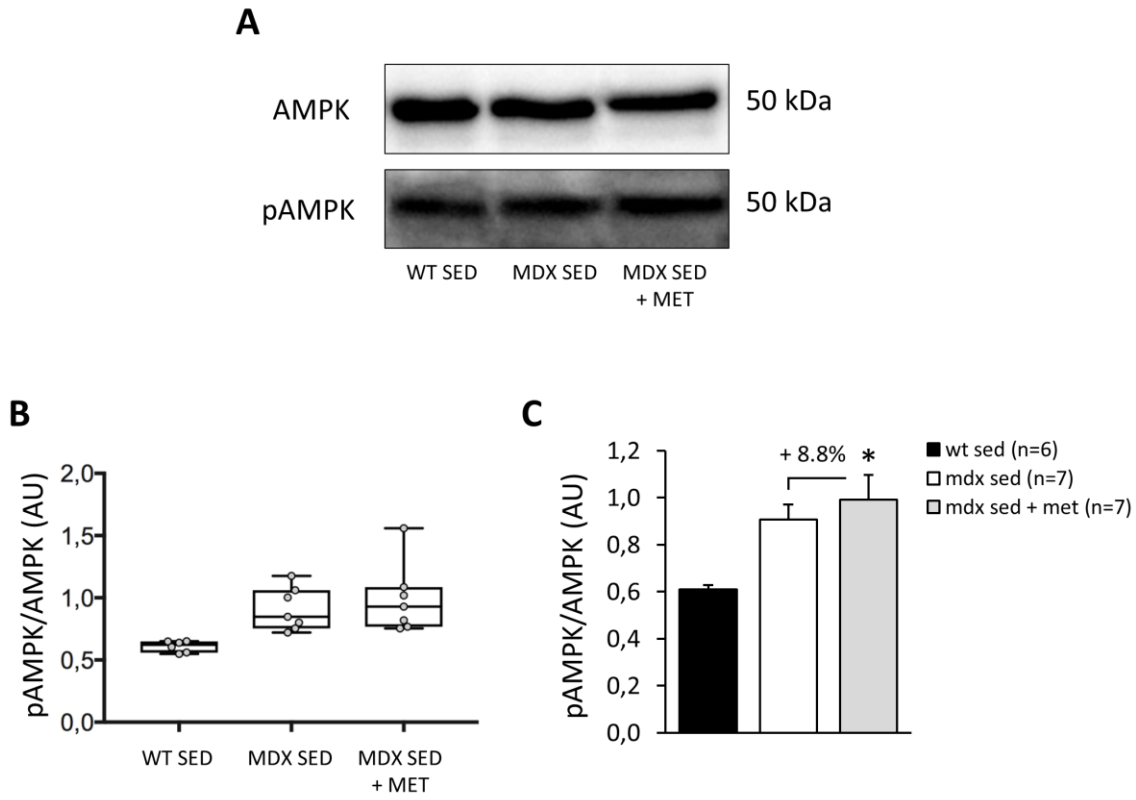

Figure 10

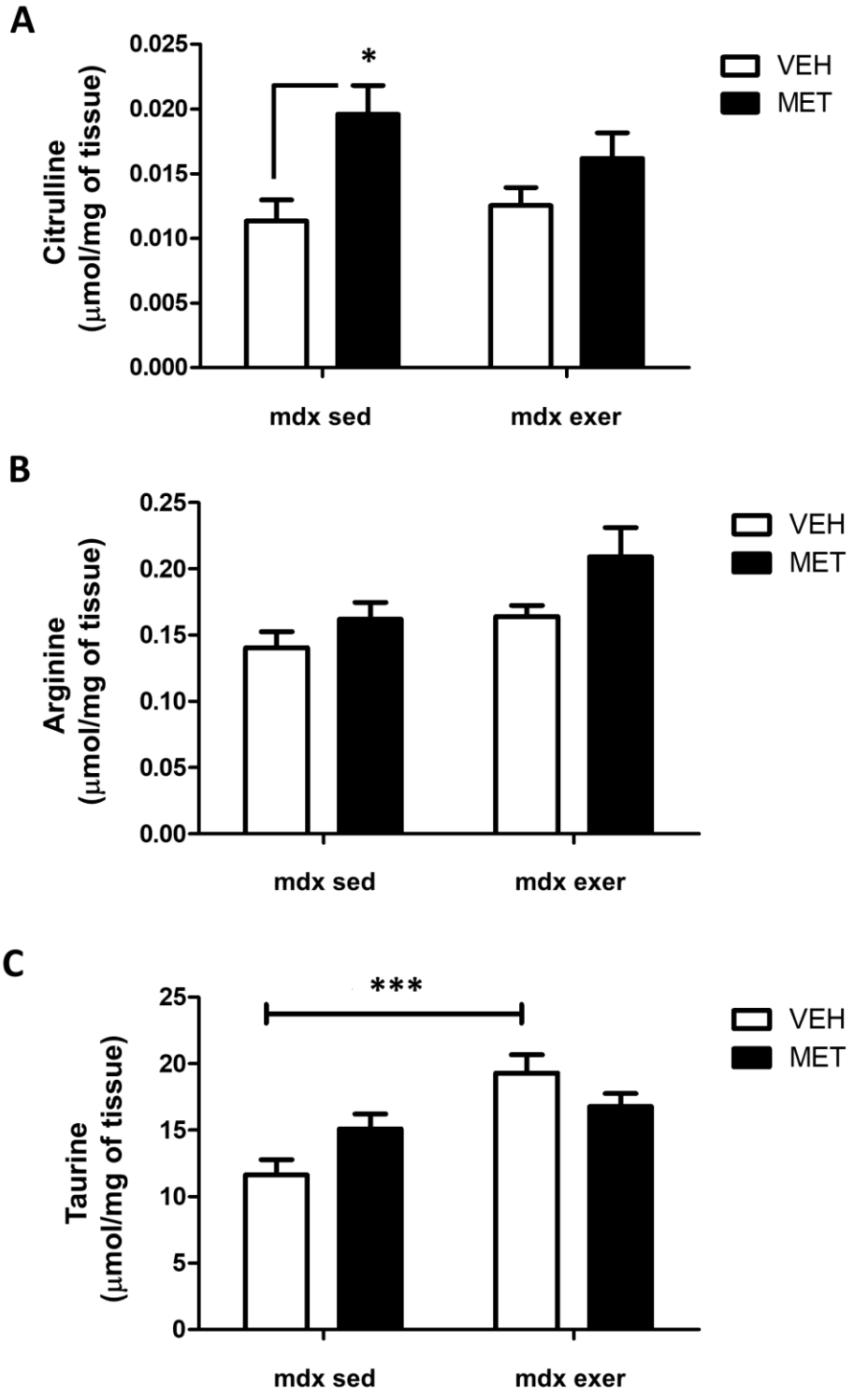

Table 1

	Diaphragm			Extensor digitorum longus				
	n	TTP (ms)	HRT (ms)	n	TTP (ms)	HRT (ms)	Eccentric force drop (10^{th} pulse)	Recovery from eccentric after 30 mins (%)
Wild type	4	30.8 ± *1.7*	24.7 ± *0.8*	5	21.6 ± *0.9*	16.8 ± *0.8*	-25 ± *13.4*	3.7 ± *13.2*
Mdx exer	6	29.8 ± *1.8*	21.1 ± *1.3*	6	20.9 ± *0.9*	16.3 ± *1.4*	-60.3 ± *6.1*	-26.7 ± *4.7*
Mdx exer + met	7	30.1 ± *0.8*	21.4 ± *0.7*	6	21.7 ± *0.3*	17 ± *1.6*	-66 ± *6.4*	-14.3 ± *25.3*

Table 1: Effect of metformin on isolated muscles kinetics and EDL eccentric contraction. In the table are shown isometric contraction kinetic parameters time to peak (TTP) and half-relaxation time (HRT), both measured in milliseconds, for diaphragm and EDL muscle in wt and treated/untreated exercised *mdx* mice. Each value is expressed as the mean ± SEM from the number of mice indicated in the column. No significant differences among groups were found by ANOVA analysis. For EDL muscle the values of eccentric contraction force drop and of the recovery of force after 30 minutes from the last eccentric stimulation are reported. A significant difference among groups was found for eccentric contraction force drop: a significant difference among groups was found by ANOVA analysis ($F = 5.2$, $p < 0.03$).

Table 2

	n	Liver (mg/g)	Heart (mg/g)	Kidney (mg/g)	Spleen (mg/g)	Plasma glucose (% variation vs WT)
Wild type	6	42.9 ± *3.1*	5.1 ± *0.3*	6.9 ± *0.3*	3.4 ± *0.3*	–
Mdx sed	8	52 ± *1.5*	4.9 ± *0.2*	7.6 ± *0.3*	3.6 ± *0.2*	+ 10%
Mdx sed + met	7	50.2 ± *1.7*	4.4 ± *0.09*	7.3 ± *0.2*	3.5 ± *0.1*	+ 9%
Mdx exer	6	51.1 ± *1.5*	5.8 ± *0.3*	7.6 ± *0.1*	3.6 ± *0.1*	- 21%
Mdx exer + met	7	57.1 ± *1.1*	4.7 ± *0.2*	7.8 ± *0.3*	3.2 ± *0.2*	+ 6%

Table 2: Effect of metformin on vital organs and plasma glucose concentration. The table shows the weights of vital organs (liver, heart, kidney and spleen), normalized on the body weight of each mouse (mg/g). Each value is expressed as the mean ± SEM from the number of mice indicated in the column. For all the organ weights, a significant difference among groups was found by ANOVA analysis ($F > 3.65$, $p < 0.005$). Bonferroni post hoc for individual differences between groups are as follows: significantly different vs °vs mdx exer ($p < 0.004$).